

Supporting Information for

Synthesis and Coordination Chemistry of Tridentate (PNN) Amine Enamido Phosphine Ligands with Ruthenium

Truman C. Wambach, Carsten Lenczyk, Brian O. Patrick, and Michael D. Fryzuk

*Department of Chemistry, The University of British Columbia, 2036 Main Mall, Vancouver BC,
Canada V6R 1Z1*

Index:

X-ray crystallography	S3
Additional Experimental Details	S4
Multinuclear NMR Spectra	
¹ H NMR of 1	S8
¹³ C NMR of 1	S9
¹ H- ¹³ C HSQC of 1	S10
¹ H- ¹ H COSY of 1	S11
¹ H NMR of 2a	S12
¹³ C NMR of 2a	S13
¹ H- ¹³ C HSQC of 2a	S14
¹ H- ¹ H COSY of 2a	S15
¹ H NMR of 2b	S16
¹³ C NMR of 2b	S17
¹ H- ¹³ C HSQC of 2b	S18
¹ H- ¹ H COSY of 2b	S19
¹ H NMR of 3a	S20
¹³ C NMR of 3a	S21
¹ H- ¹³ C HSQC of 3a	S22

^1H - ^1H COSY of 3a	S23
ATR-FTIR of 3a	S24
^1H NMR of 3b	S25
^{13}C NMR of 3b	S26
^1H - ^{13}C HSQC of 3b	S27
^1H - ^1H COSY of 3b	S28
ATR-FTIR of 3b	S29
^1H NMR of 4a	S30
^{13}C NMR of 4a	S31
^1H - ^{13}C HSQC of 4a	S32
^1H - ^1H COSY of 4a	S33
ATR-FTIR of 4a	S34
^1H NMR of 4b	S35
^{13}C NMR of 4b	S36
^1H - ^{13}C HSQC of 4b	S37
^1H - ^1H COSY of 4b	S38
ATR-FTIR of 4b	S39
^1H NMR of 5	S40
^{13}C NMR of 5	S41
^1H - ^{13}C HSQC 5	S42
ATR-FTIR of 5	S43

Compound	4a
Empirical formula	C ₂₀ H ₃₈ N ₂ OPRu
Formula weight [g/mol]	454.56
Color / Morphology	red / rectangular prism
Crystal size [mm]	0.120, 0.150, 0.300
Temperature [K]	100
Wavelength [Å]	0.71069 (Mo-K α)
Crystal system	monoclinic
Space group	P2 ₁ /m
<i>a</i> [Å]	9.6117(8)
<i>b</i> [Å]	11.6787(2)
<i>c</i> [Å]	10.5243(2)
α, β, γ [°]	90, 111.025(2), 90
<i>V</i> (Å ³)	11.02.72(2)
$\rho_{\text{calc.}}$ [g cm ⁻³]	1.369
<i>Z</i>	2
<i>F</i> (000)	478.0
μ [mm ⁻¹]	0.794
<i>T</i> _{max} / <i>T</i> _{min}	0.909, 0.867
<i>hkl</i> range	-12 ≤ <i>h</i> ≤ 12, -15 ≤ <i>k</i> ≤ 15, -13 ≤ <i>l</i> ≤ 13
θ range [°]	2.073-27.924
Independent reflections, <i>R</i> _{int}	2769, 0.0293
Completeness to θ_{max} (%)	99.9
Absorption correction	Multi-scan (SADABS)
Refinement Method	Full-matrix least-squares on <i>F</i> ²
Measured reflections	11859
Data / restraints / parameters	2769 / 212 / 185
Goodness-of-fit	1.048
<i>RI</i> , <i>wR2</i> (<i>I</i> > 2 σ (<i>I</i>))	0.0244, 0.0560
<i>RI</i> , <i>wR2</i> (all data)	0.0298, 0.0586
Residual electron dens. [e Å ⁻³]	-0.41 / 0.40

Reaction of **RuH**{(PNN)^{But}}**(CO)** (**4a**) with H₂. A solution of **4a** (0.013 g, 0.028 mmol) dissolved in C₆D₆ (0.5 ml) was added to a flame-sealable NMR tube sealed with a Kontes valve. The solution was freeze-pump-thaw degassed three times under high vacuum and subsequently frozen in liquid nitrogen. The headspace was evacuated for a final time, and was then backfilled with H₂ to 0.95 atm of pressure while frozen in liquid nitrogen. The NMR tube, submerged in liquid nitrogen, was sealed with a torch and subsequently allowed to warm to room temperature in a safe location. Monitoring the reaction by ¹H and ³¹P{¹H} NMR spectroscopy showed no reaction within 7 days. Heating the mixture to 60 °C, and then 80 °C resulted in no change. Upon heating to 100 °C for 24 hours, 13 % conversion to a new ³¹P{¹H} resonance at δ 32.2 (s) occurred. At this point, the ¹H NMR spectrum showed no new hydride resonances.

Reaction of **RuH**{(PNN)^{Pr}}**(CO)** (**4b**) with H₂. A solution of **4b** (0.030 g, 0.070 mmol) dissolved in C₆D₆ (0.5 ml) was placed as a solution in a flame-sealable NMR tube sealed with a Kontes valve. The solution was freeze-pump-thaw degassed three times under high vacuum and subsequently frozen in liquid nitrogen; the headspace was evacuated for a final time then backfilled with H₂ to 0.95 atm while still frozen in liquid nitrogen. The NMR tube, submerged in liquid nitrogen, was sealed with a torch and allowed to warm to room temperature in a safe location. Monitoring the reaction by ¹H and ³¹P{¹H} NMR after 1 hour shows a signal at δ 104.7, corresponding to an intermediate in the reaction and a smaller set of resonances at δ 90.5 (d, ²J_{PP} = 6.9 Hz) and 79.0 (d, ²J_{PP} = 6.9 Hz) corresponding to the final product. The largest signal observed at this point is **4b**. Allowing the reaction to proceed for 13 hours gives a ratio of peaks of 1.8 : 1.0 : 1.0 : 6.6 corresponding to the resonances at δ 104.7 : 90.6 : 79.0 : 76.4 (**4b**). After 10 days, the mixture mostly corresponds to the resonances at δ 90.6 and 79.0. Multinuclear NMR spectra were recorded at this time and diagnostic features are reported below. ³¹P{¹H} NMR (C₆D₆, 161.9 MHz, 298 K): δ 79.0 (d, ²J_{PP} = 6.9 Hz), 90.5 (d, ²J_{PP} = 6.9 Hz). ¹H NMR (C₆D₆, 400 MHz, 298 K): δ -10.6 (br.d, J = 18.5 Hz), -10.5 (ddd, J_{HH} = 6.6 Hz, J_{PH} = 14.3 Hz, J_{PH} = 23.0 Hz), - 8.5 (dt, J = 5.4 Hz, J = 11.8 Hz).

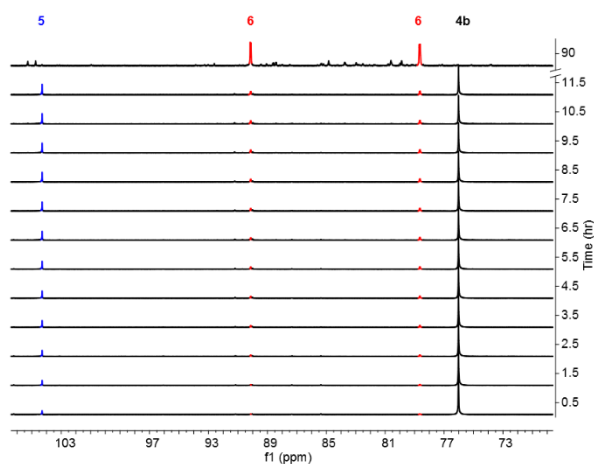


Figure S1: ³¹P{¹H} NMR spectra recorded to monitor the conversion of **4b** to new products under H₂.

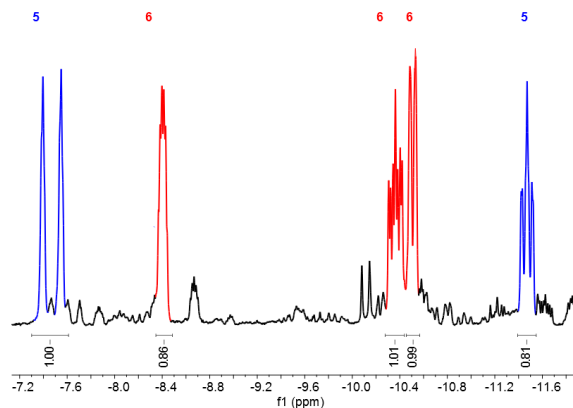


Figure S2: The hydride region of the ¹H NMR spectrum recorded during conversion of **4b** to **5** and **6**.

Synthesis of spectroscopically pure $(\text{PNN})^{\text{Pr}}(\text{D})$ ($\mathbf{2b}^*$). KH (0.167 g, 4.2 mmol) was added to a scintillation vial equipped with a stir bar and suspended in THF (4 ml). To the stirred solution of KH was added $(\text{PNN})^{\text{Pr}}(\text{H})$ ($\mathbf{2b}$) (0.257 g, 0.86 mmol) was added, the reaction was allowed to stir for 24 hours at ambient temperature. during this time the color of the solution changed from colorless to yellow-green. The excess KH was removed by filtration through a glass fiber filter packed into a pipette. The filtrate was added to a Schlenk flask, removed from the glovebox and immediately quenched with MeOD (~ 3 ml), which resulted in instantaneous formation of a colorless solution. The volatiles were removed under vacuum. In the glovebox the resulting paste was extracted with pentane (10 ml) and filtered through a glass fiber filter. The volatiles were removed under vacuum to give the yellow oil (0.272 g, 108%, *sample was likely not fully dry when yield was recorded*). Integration of the residual ^1H NMR resonances assigned to the N-H proton indicates 94% incorporation of deuterium.

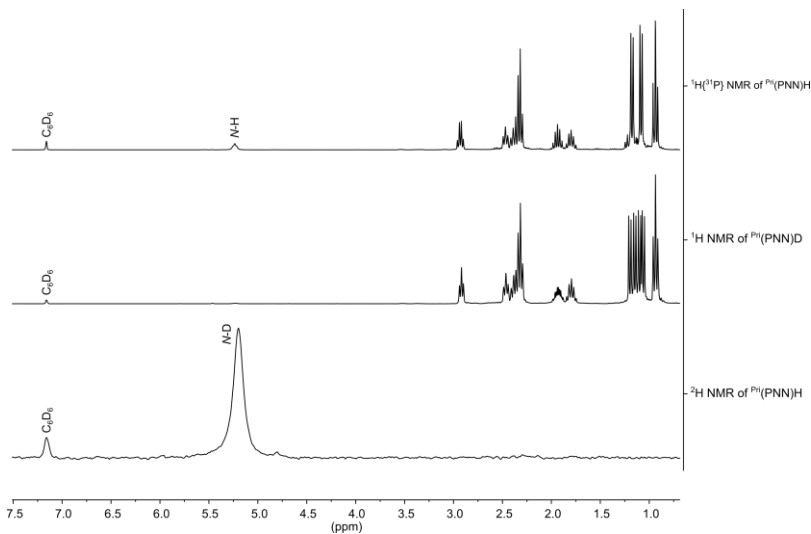


Figure S3: Multinuclear NMR spectra of $(\text{PNN})\text{H}$ ($\mathbf{2b}$) and $(\text{PNN})\text{D}$ ($\mathbf{2b}^*$) in C_6D_6

Synthesis of $\text{RuHCl}\{(\text{PNN})^{\text{Pr}}(\text{D})\}(\text{CO})$ ($\mathbf{3b}^*$). To a scintillation vial was added $\text{RuHCl}(\text{P}^i\text{Pr}_3)_2(\text{CO})$ (0.252 g, 0.518 mmol) as well as a slight excess of $\mathbf{2b}^*$ (0.196 g, 0.654 mmol). Diethyl ether (10 ml) was added to the vial and the mixture was stirred for 1 week at which point a yellow suspension formed. The reaction was cooled to -32°C for 30 minutes, and was subsequently filtered through sinter glass filter. The yellow solids were washed with cold diethyl ether (2x ~2 ml) to give a white powder (0.160g, 67%).

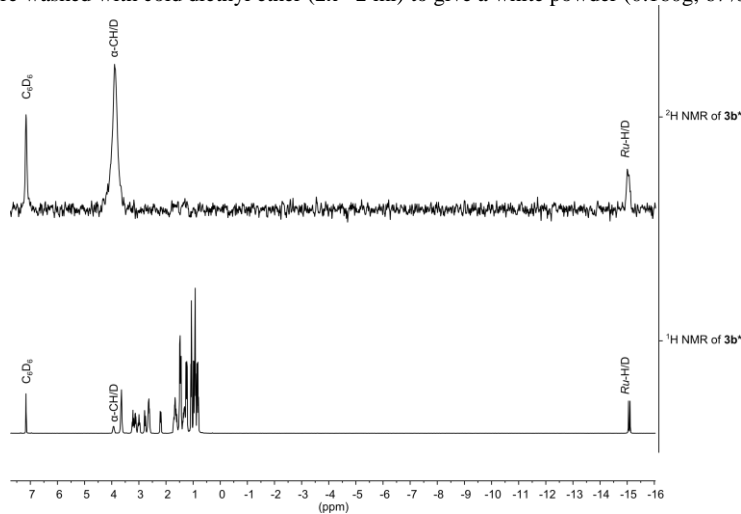


Figure S4: Multinuclear NMR spectra of $\text{Ru}(\text{H}/\text{D})\text{Cl}\{(\text{PNN})\text{H}/\text{D}\}(\text{CO})$ ($\mathbf{3b}^*$) showing deuterium scrambling in to the $\alpha\text{-CH}/\text{D}$ and $\text{Ru-H}/\text{D}$ positions.

Catalytic AD of Benzyl Alcohol to Benzyl Benzoate using $\text{RuH}\{\text{PNN}^{\text{But}}\}(\text{CO})$ (**4a**) and $\text{RuH}\{\text{PNN}^{\text{Pri}}\}(\text{CO})$ (**4b**).

- a) **4a** (0.019 g, 0.041 mmol) was dissolved in a 1.0 M solution of mesitylene in *d*₈-toluene (0.50 ml) in the glove box in a J. Young tube. Using Schlenk techniques, benzyl alcohol (0.43 ml, 4.1 mmol) was added. The mixture was shaken then the J. Young tube was opened to the Ar manifold of the Schlenk line and heated to 110 °C. The reaction was monitored intermittently by ¹H NMR spectroscopy to determine the percent conversion.

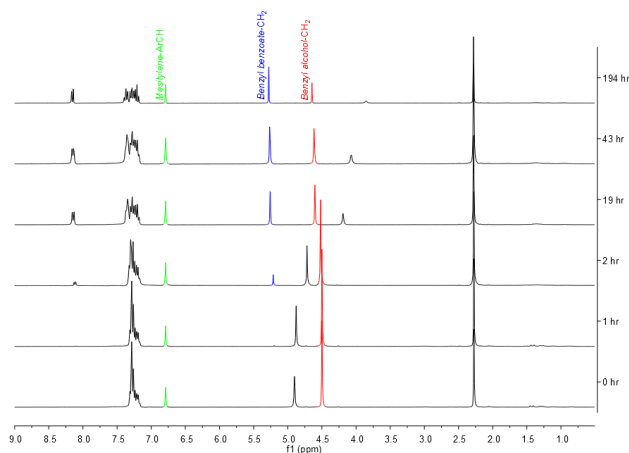


Figure S5: ¹H NMR spectra recorded while monitoring the conversion of benzyl alcohol to benzyl benzoate using **4a** as a catalyst.

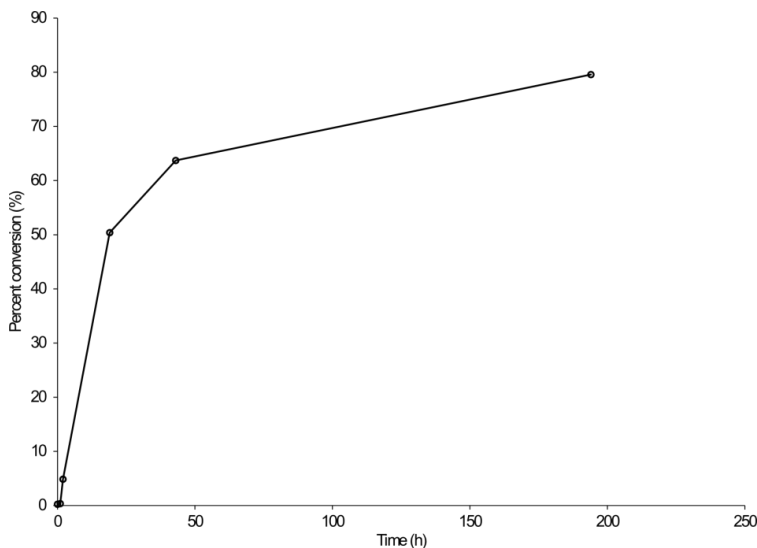


Figure S6: Catalytic conversion of benzyl alcohol to benzyl benzoate in a J. Young tube vented to an Ar manifold.

b) In the glove box **4a** or **4b** (0.0100 mmol) was added to a two neck flask (100 ml) equipped with a medium stir bar and a Schlenk arm gas inlet. Mesitylene (0.070 ml, 5.0 mmol) was added as an internal standard along with toluene (2.00 ml). The Schlenk flask was sealed and removed from the glove box. On the Schlenk line, benzyl alcohol (1.04 ml, 10.0 mmol) was added. The Schlenk flask was fitted with a reflux condenser, connected to an Ar manifold, and vented to a mercury bubbler through the reflux condenser. The reaction was heated to 115 °C. The reaction was sampled twice at two hour intervals for analysis by GC-FID by allowing the mixture to cool to room temperature for at least 30 min and taking samples of at least 320 μl of the reaction mixture. After sampling, the reaction was allowed to proceed. To prepare the samples for analysis by GC-FID, in open air, a sample (320 μl) was diluted in toluene (10.00 ml).

Table S1 presents ^{13}C APT NMR resonances assigned to linker carbon connected to phosphorus, as well as the CO stretching frequencies of the complexes **B**, **4a** and **4b**. The ^{13}C NMR resonances of **B** are shielded in comparison to the relevant resonances of **4a** and **4b**. The CO stretching frequencies of **4a** and **4b** are very similar to one another, but are smaller than the value recorded for **B**. One plausible rationale for the spectroscopically observed variance between these complexes could rely on differences in electron density distribution in the linker unit of these ligands, specifically, localization of electron density in the reactive linker portion of the ligand of **B**, where it cannot participate in back donation into the π^* orbitals of the CO ligand.

Table S1: ^{13}C NMR and FTIR Data for **B**, **4a** and **4b**.

Entry	Complex	Linker/ α -C δ (ppm)	$^1J_{\text{PC}}$ (Hz)	N-C _{enamide} δ (ppm)	$^2J_{\text{PC}}$ (Hz)	ν (CO) (cm^{-1})
1	B	65.3	50.3	169.1	15.1	1899
2	4a	90.0	41.3	180.2	26.0	1875
3	4b	88.7	44.1	180.6	18.4	1874

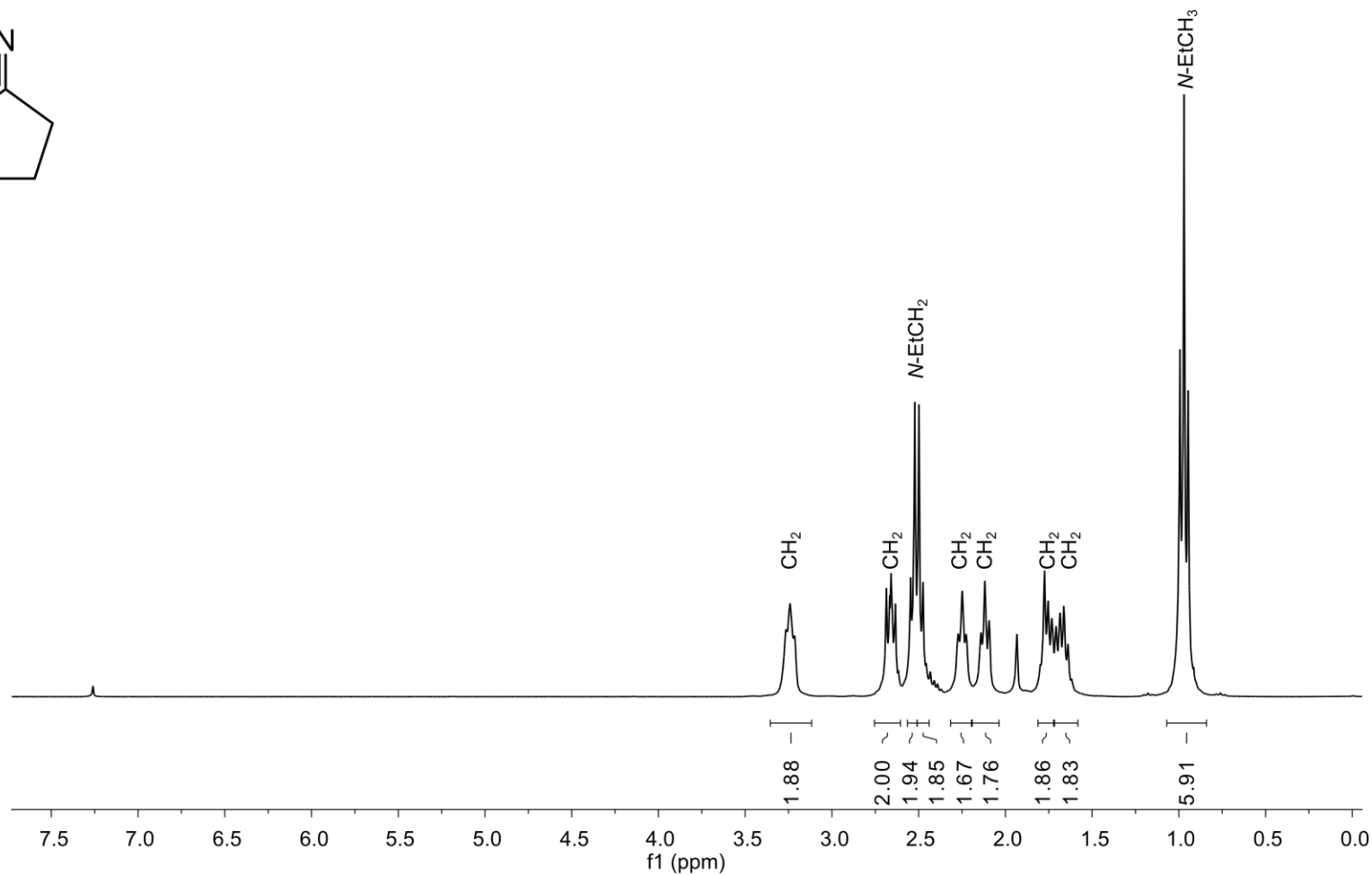
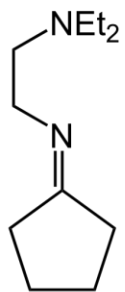


Figure S7: ¹H NMR of **1** taken at 400.0 MHz at 298 K in CDCl₃.

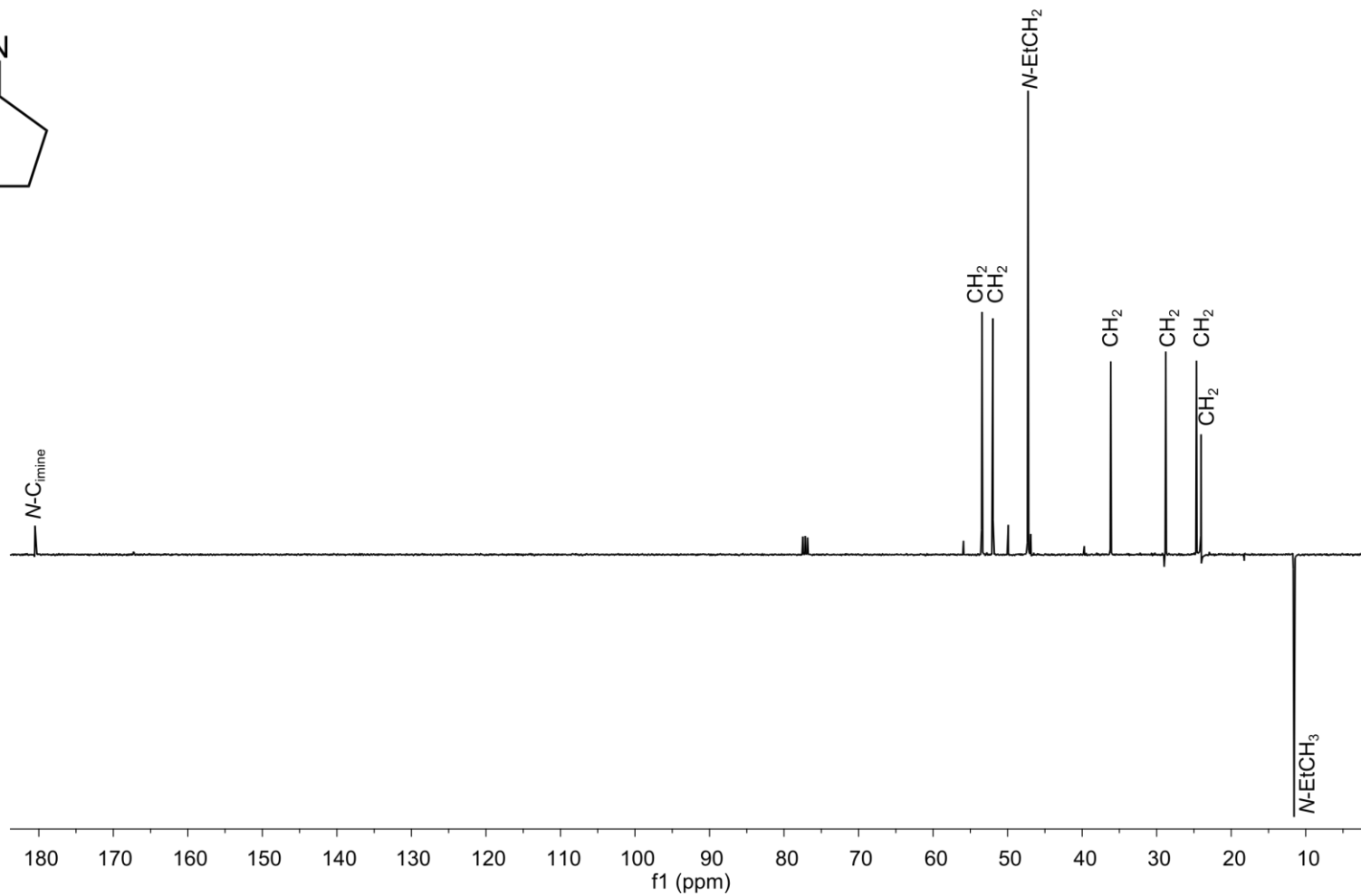
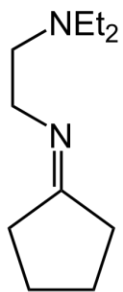


Figure S8: ^{13}C APT NMR of **1** taken at 100.6 MHz at 298 K in CDCl_3 .

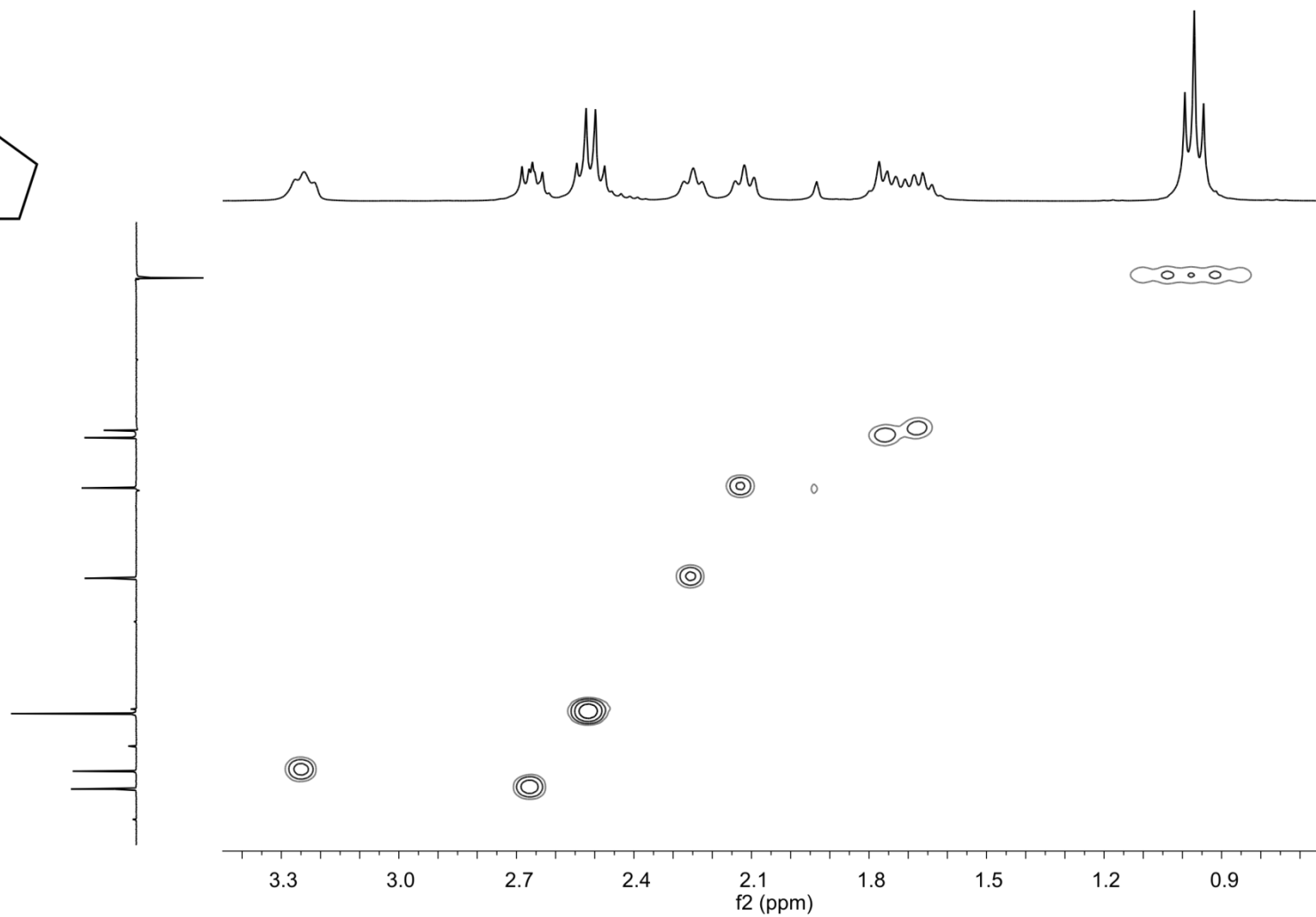
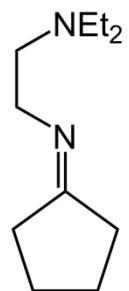


Figure S9: ^1H - ^{13}C HSQC of **1** taken at 298 K in CDCl_3 .

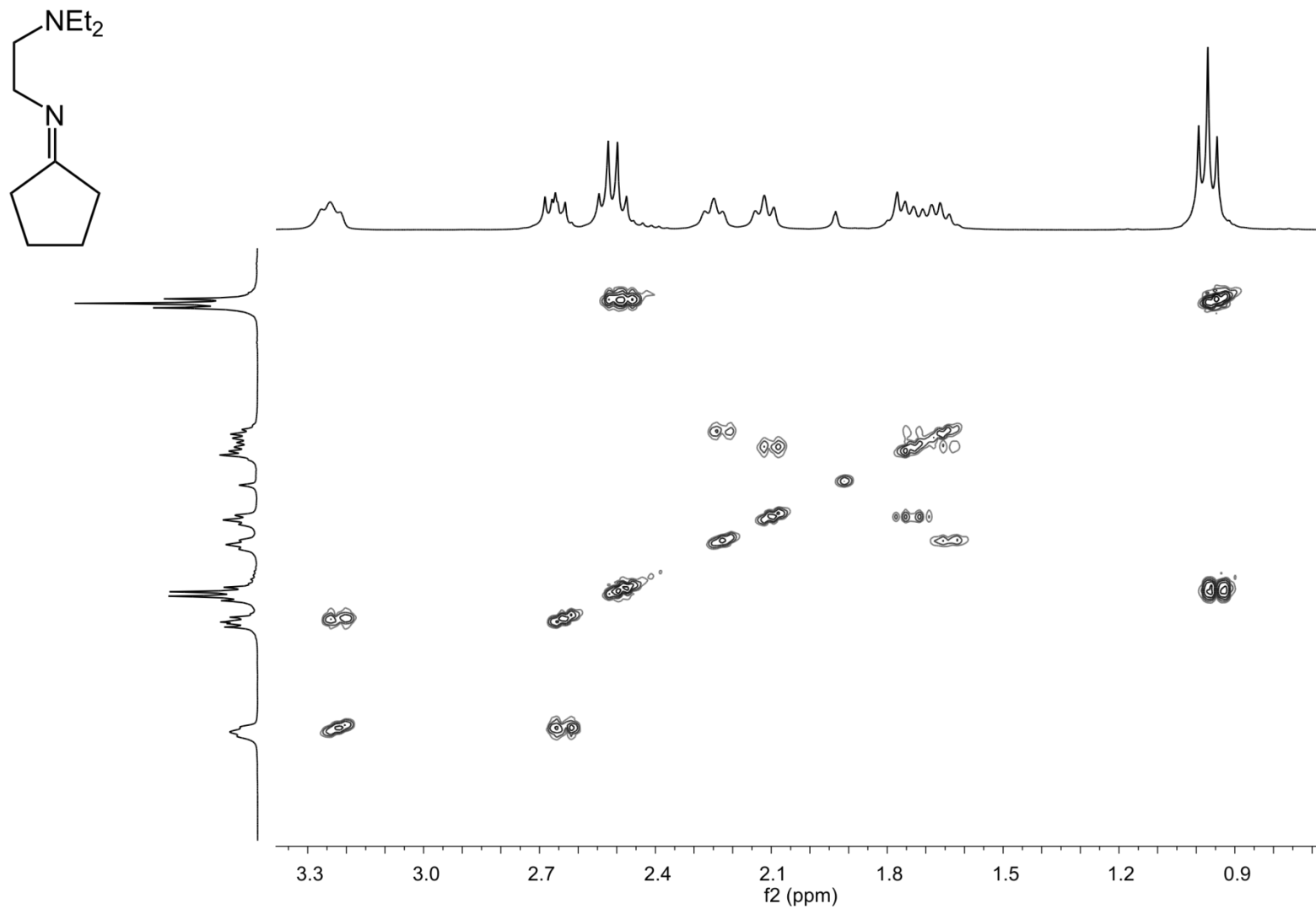
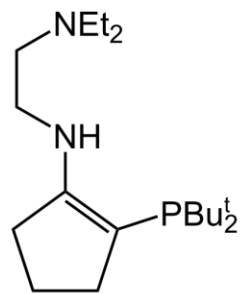


Figure S10: ^1H - ^1H COSY of **1** taken at 298 K in CDCl_3 .



$^{31}\text{P}\{^1\text{H}\}$: δ 5.8 (s)

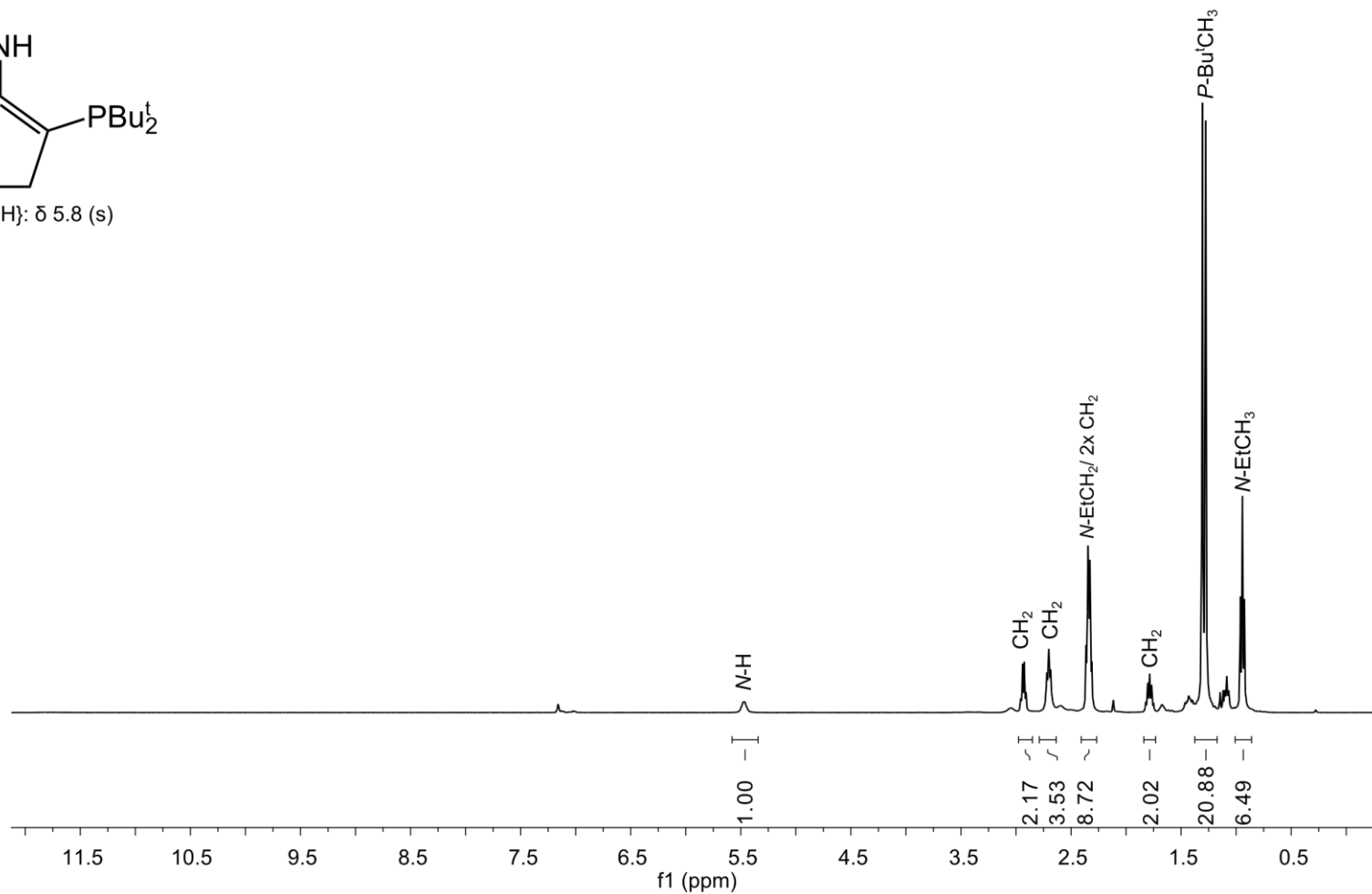


Figure S11: ^1H NMR of **2a** taken at 400.0 MHz at 298 K in C_6D_6 .

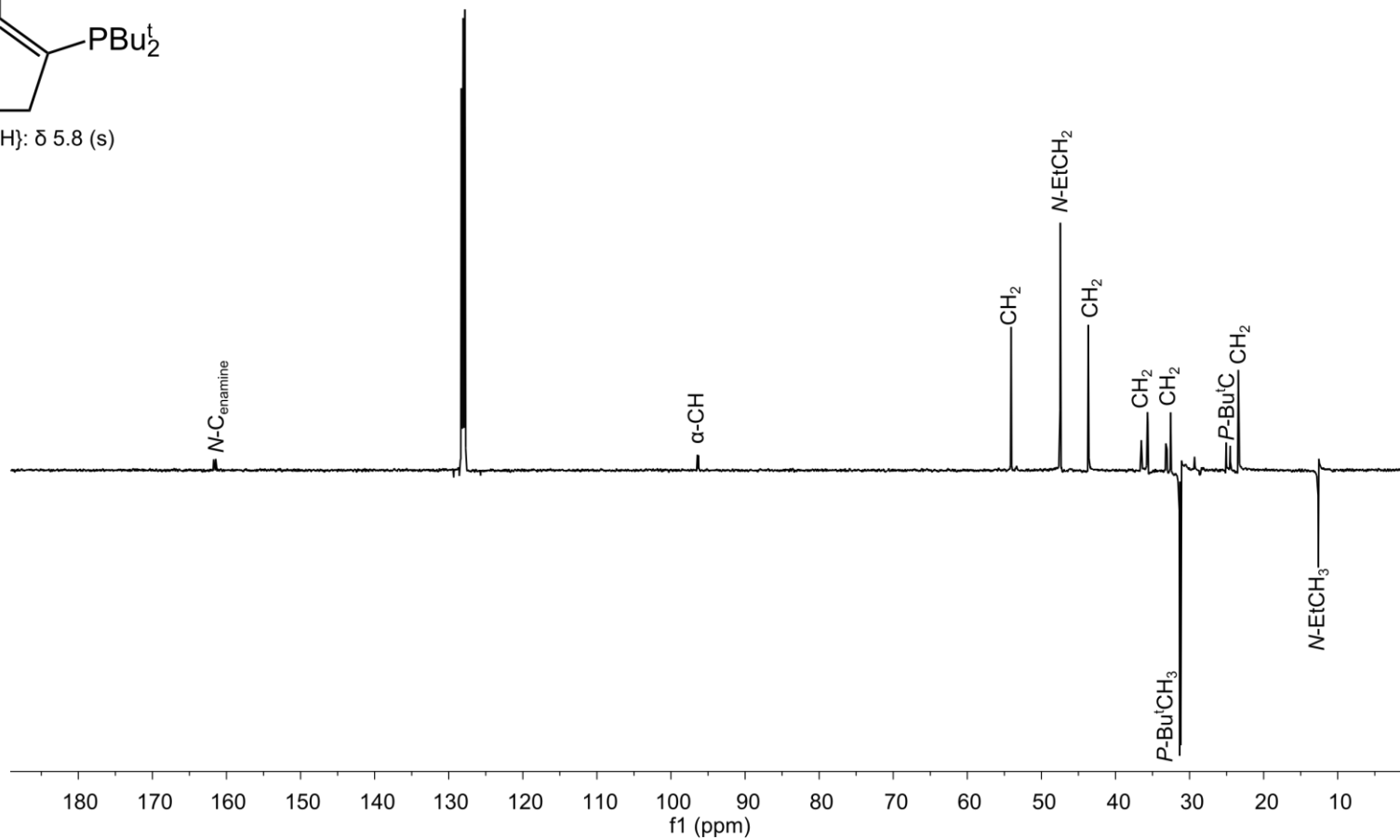
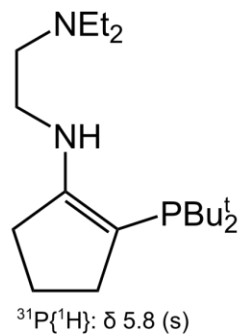


Figure S12: ^{13}C APT NMR of **2a** taken at 100.6 MHz at 298 K in C_6D_6 .

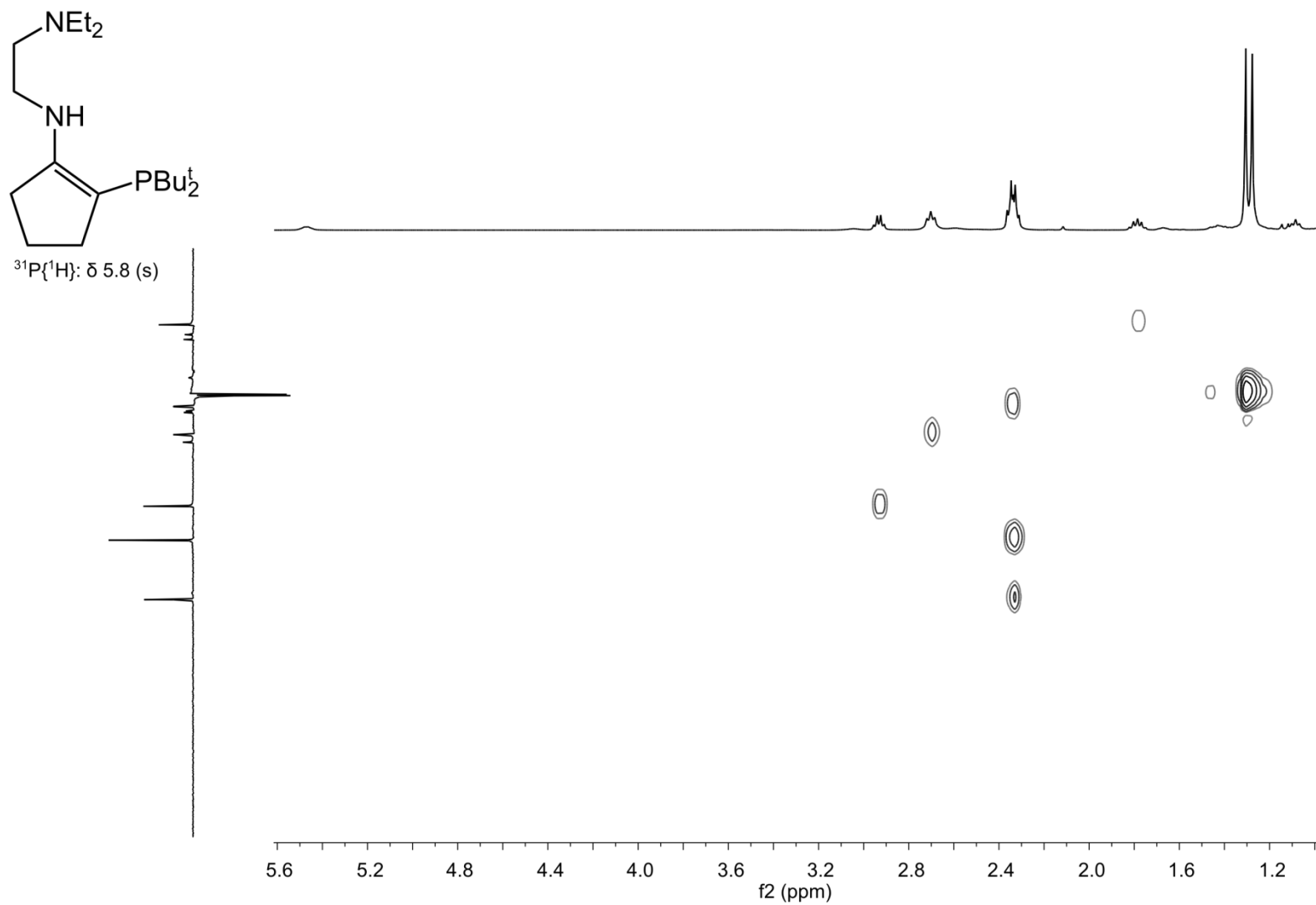


Figure S13: ^1H - ^{13}C HSQC of **2a** taken at 298 K in C_6D_6 .

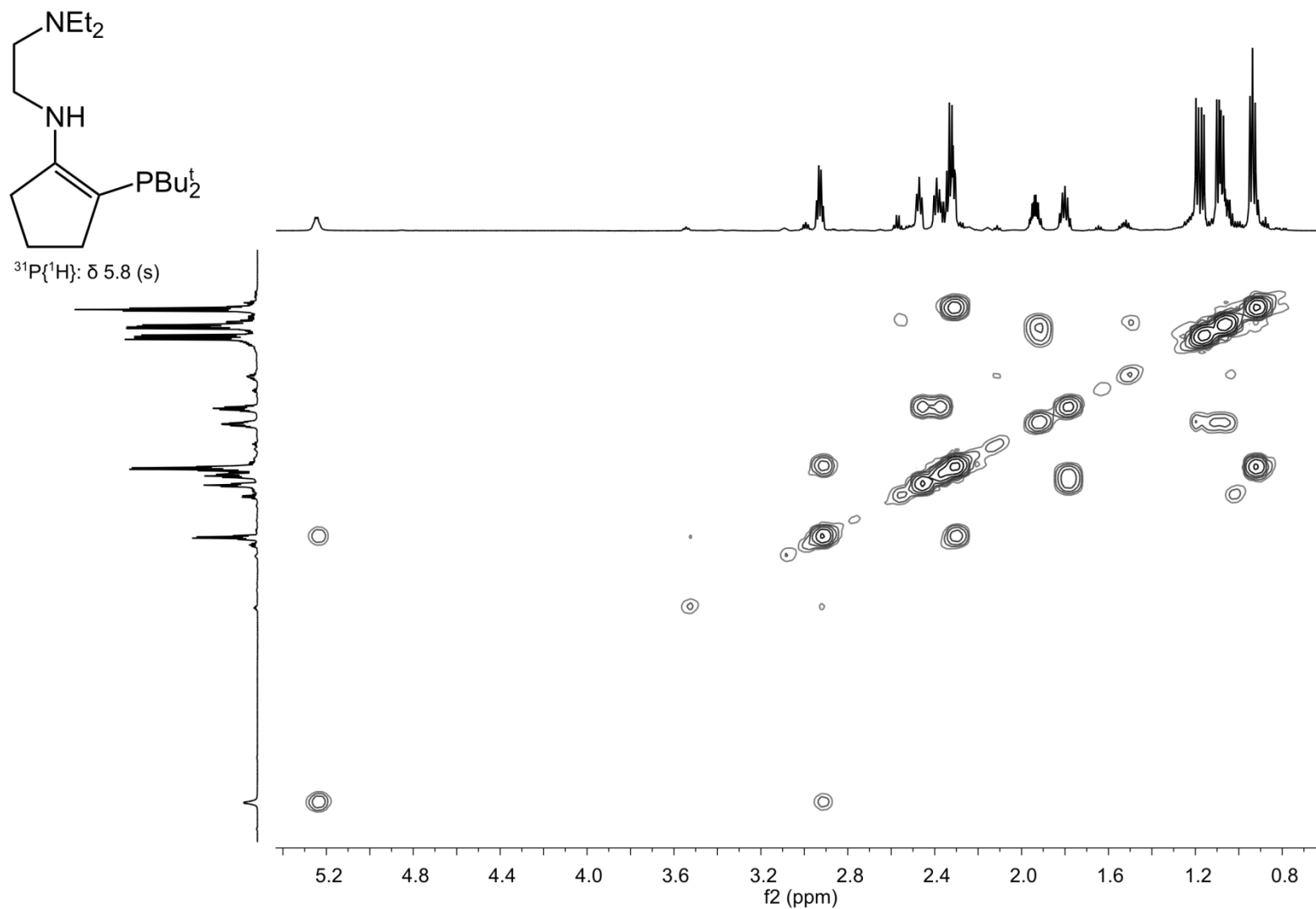
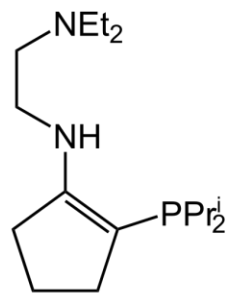


Figure S14: ^1H - ^1H COSY of **2a** taken at 298 K in C_6D_6 .



$^{31}\text{P}\{^1\text{H}\}$: δ -18.6 (s)

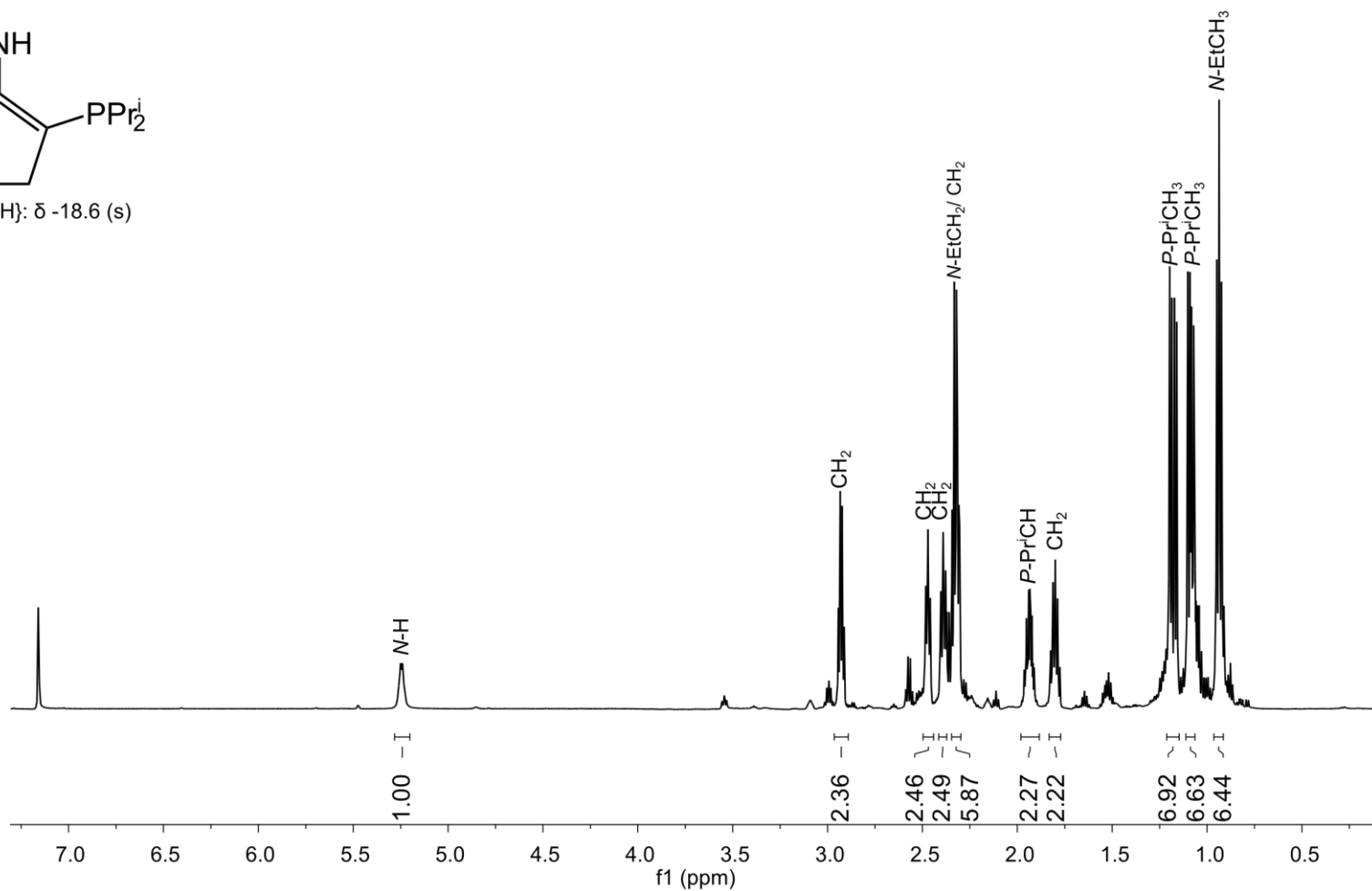


Figure S15: ^1H NMR of **2b** taken at 400.0 MHz at 298 K in C_6D_6 .

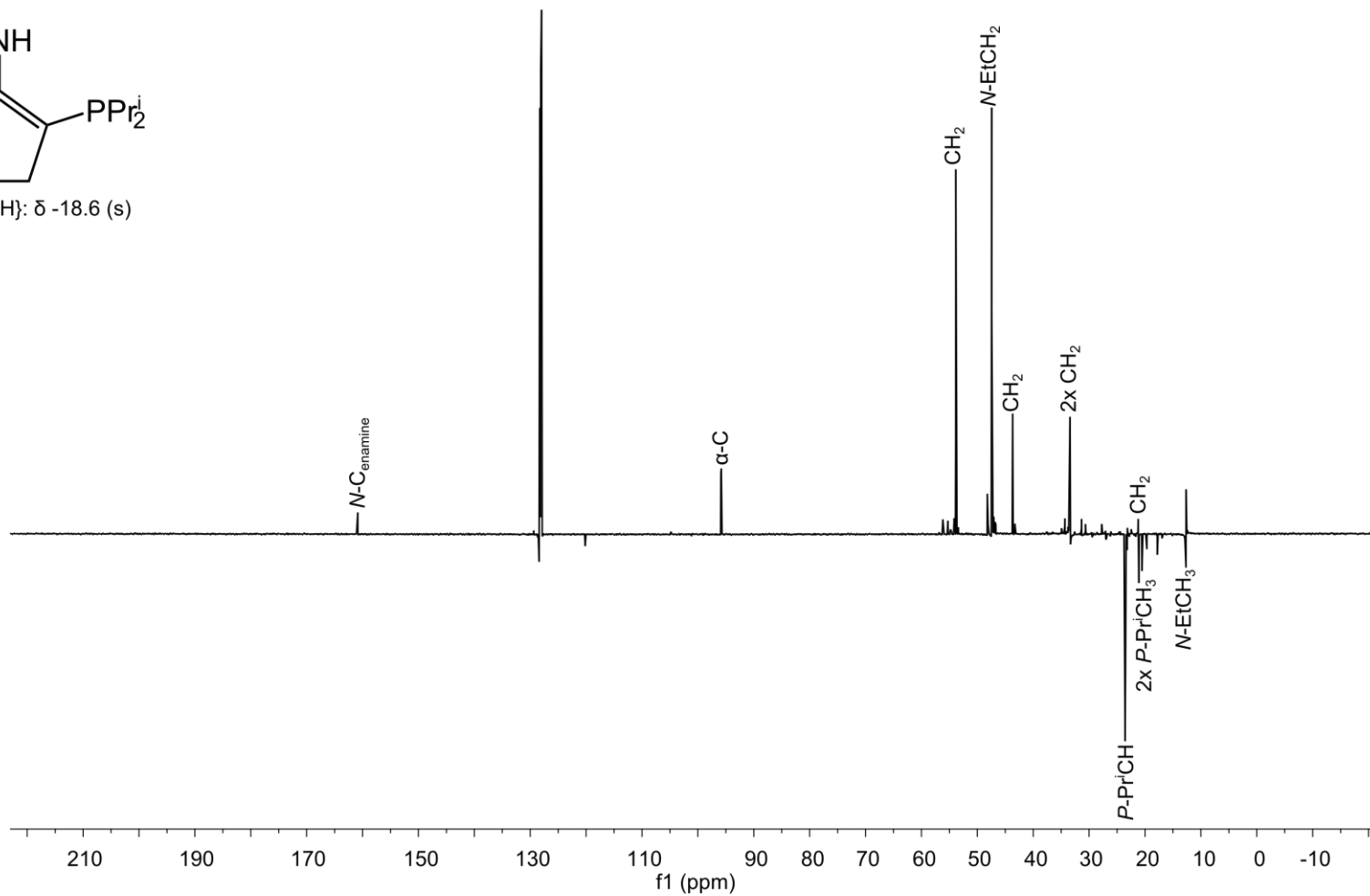
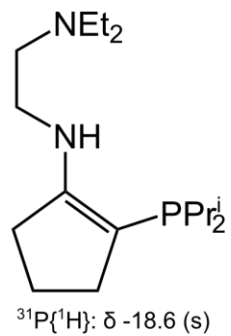
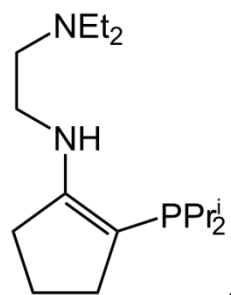


Figure S16: ^{13}C APT NMR of **2b** taken at 100.6 MHz at 298 K in C_6D_6 .



³¹P{¹H}: δ -18.6 (s)

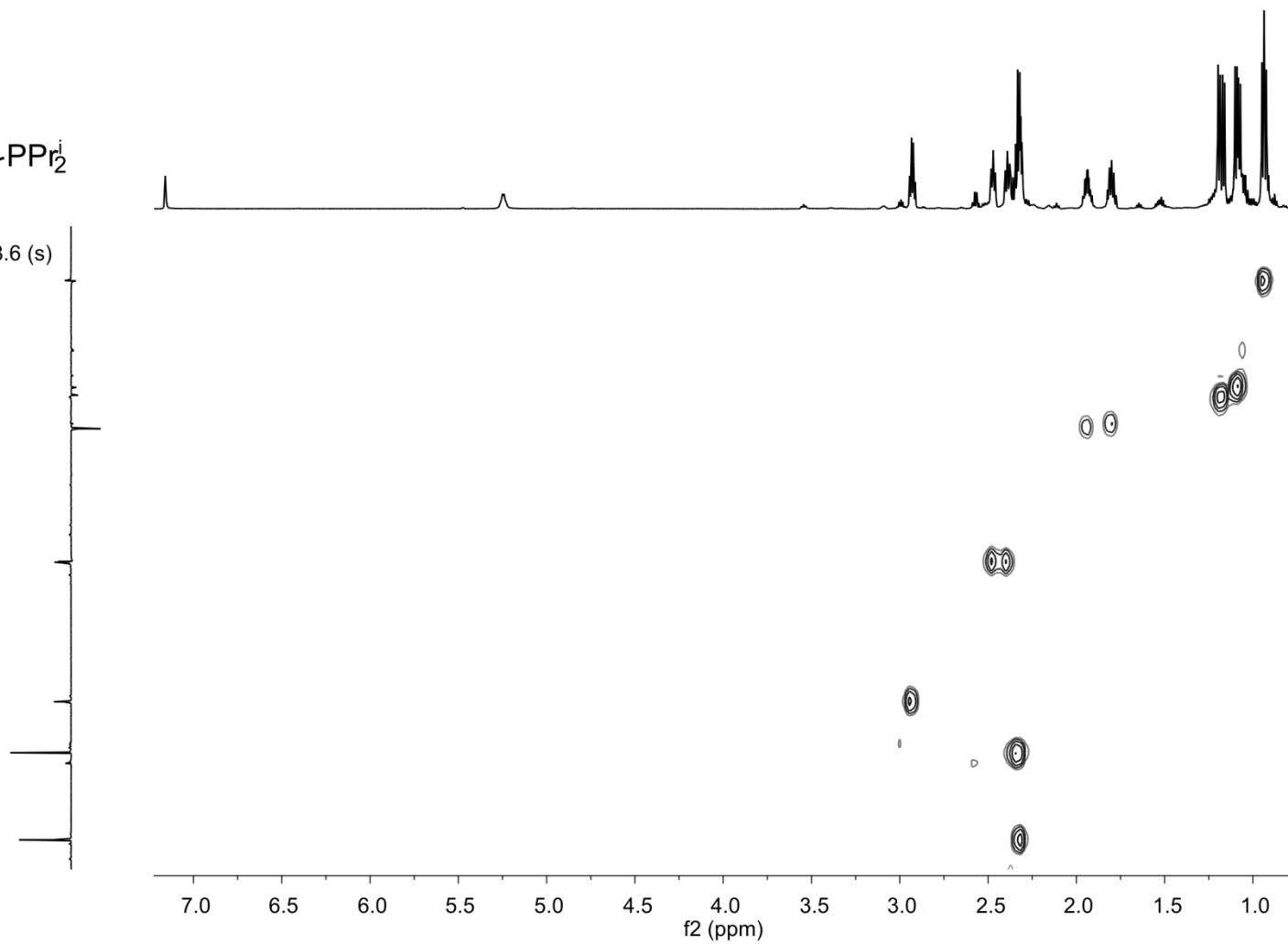


Figure S17: ¹H-¹³C HSQC of **2b** taken at 298 K.

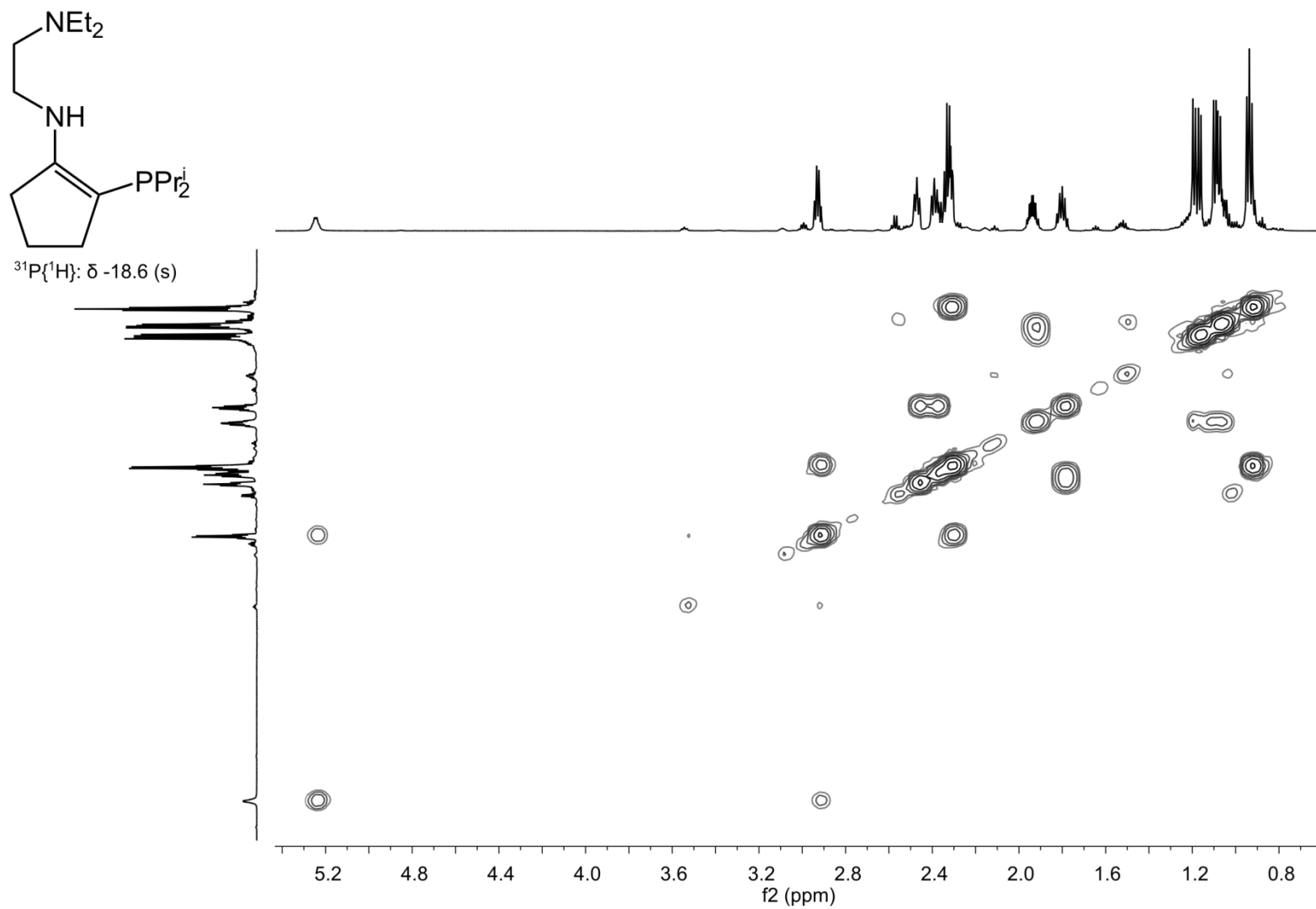


Figure S18: ^1H - ^1H COSY of **2b** taken at 298 K in C_6D_6 .

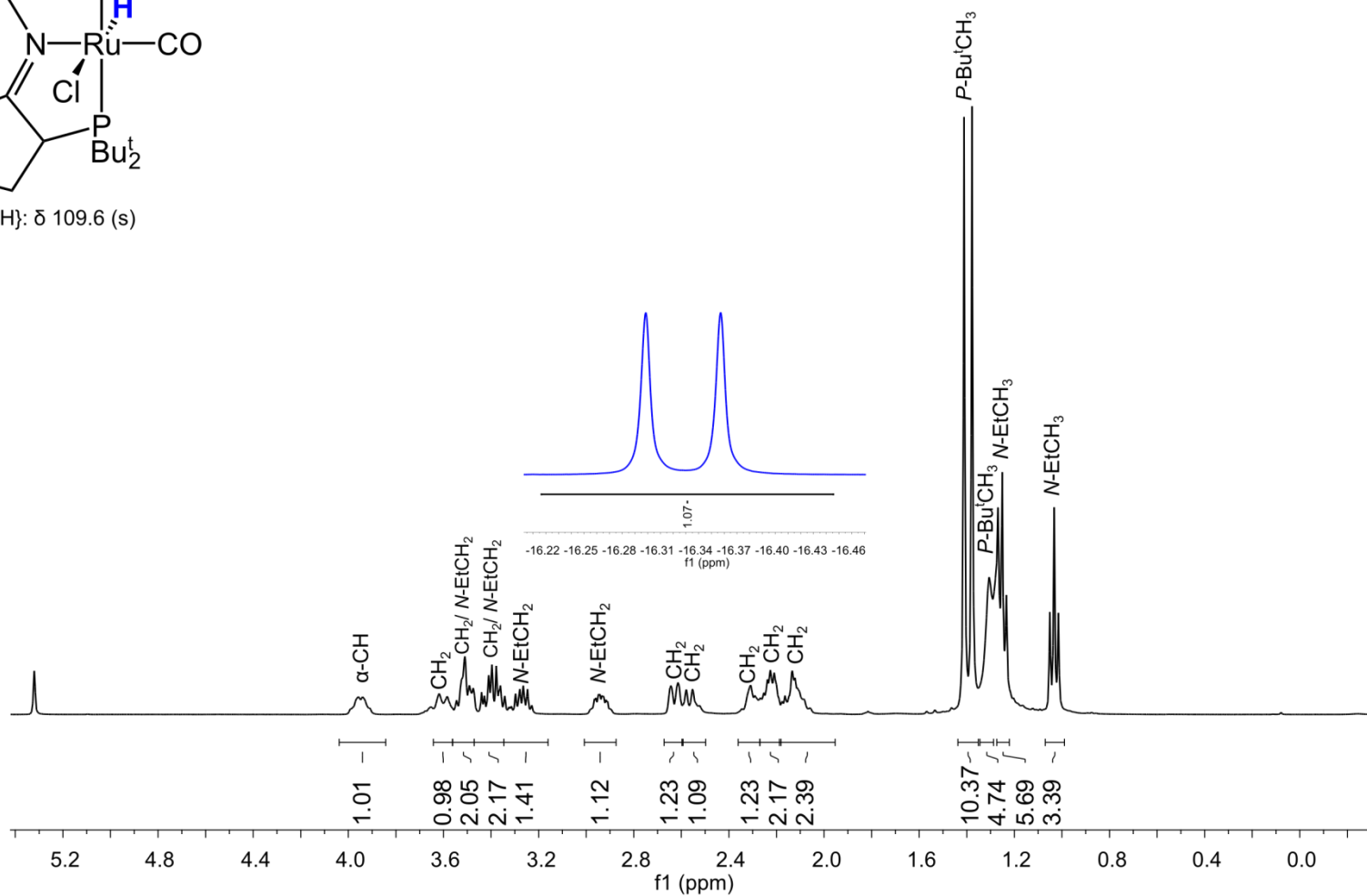
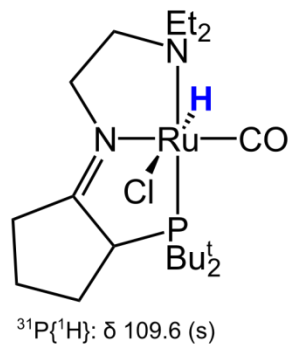


Figure S19: ^1H NMR of **3a** taken at 400.0 MHz at 298 K in CD_2Cl_2 .

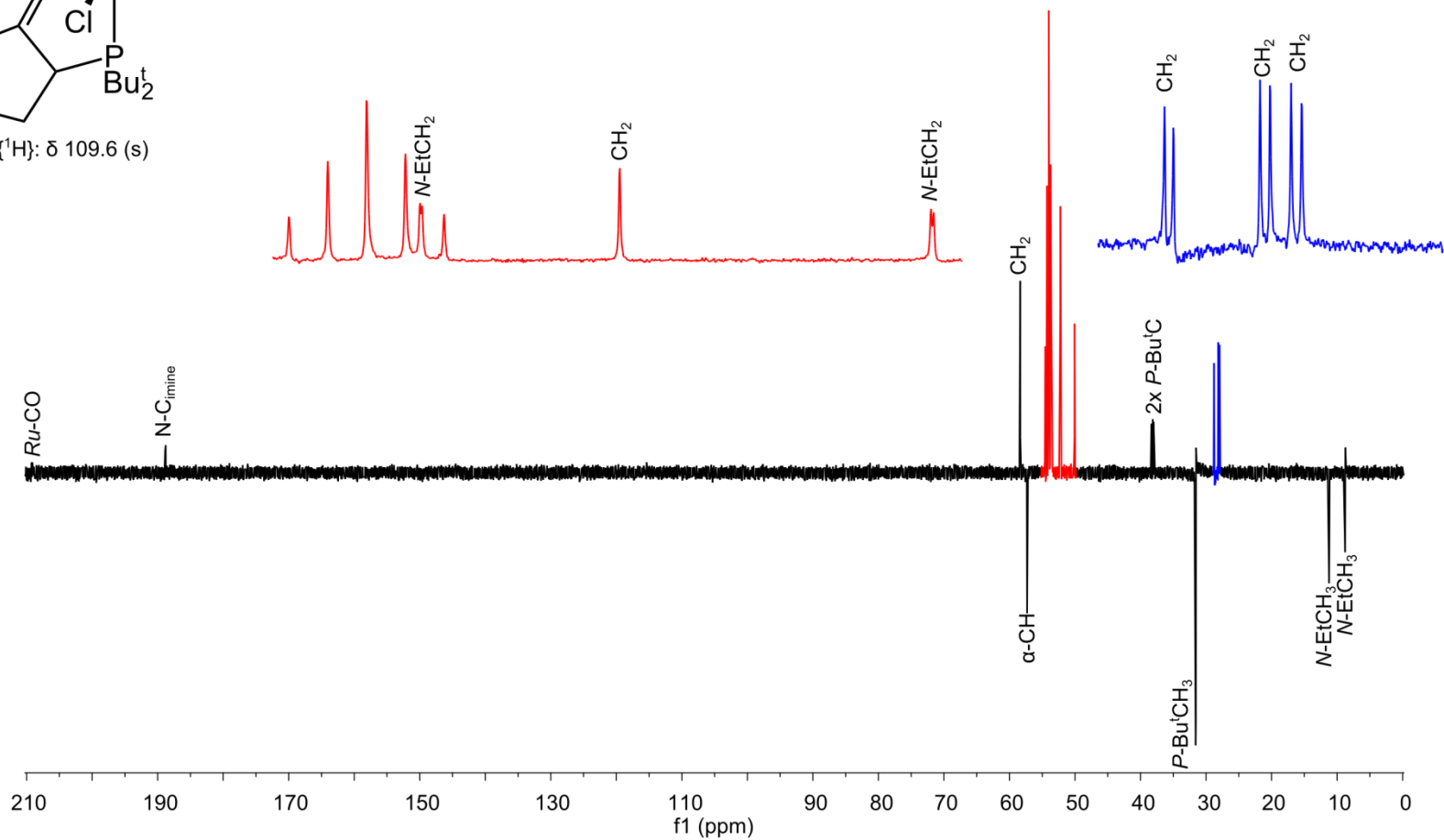
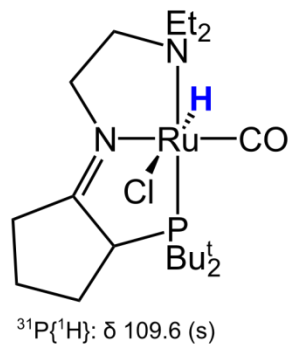
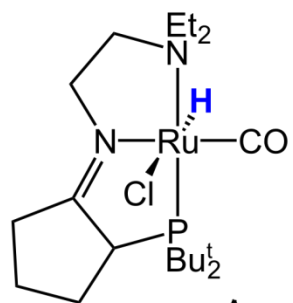


Figure S20: ^{13}C APT NMR of **3a** taken at 100.6 MHz at 298 K in CD_2Cl_2 .



³¹P{¹H}: δ 109.6 (s)

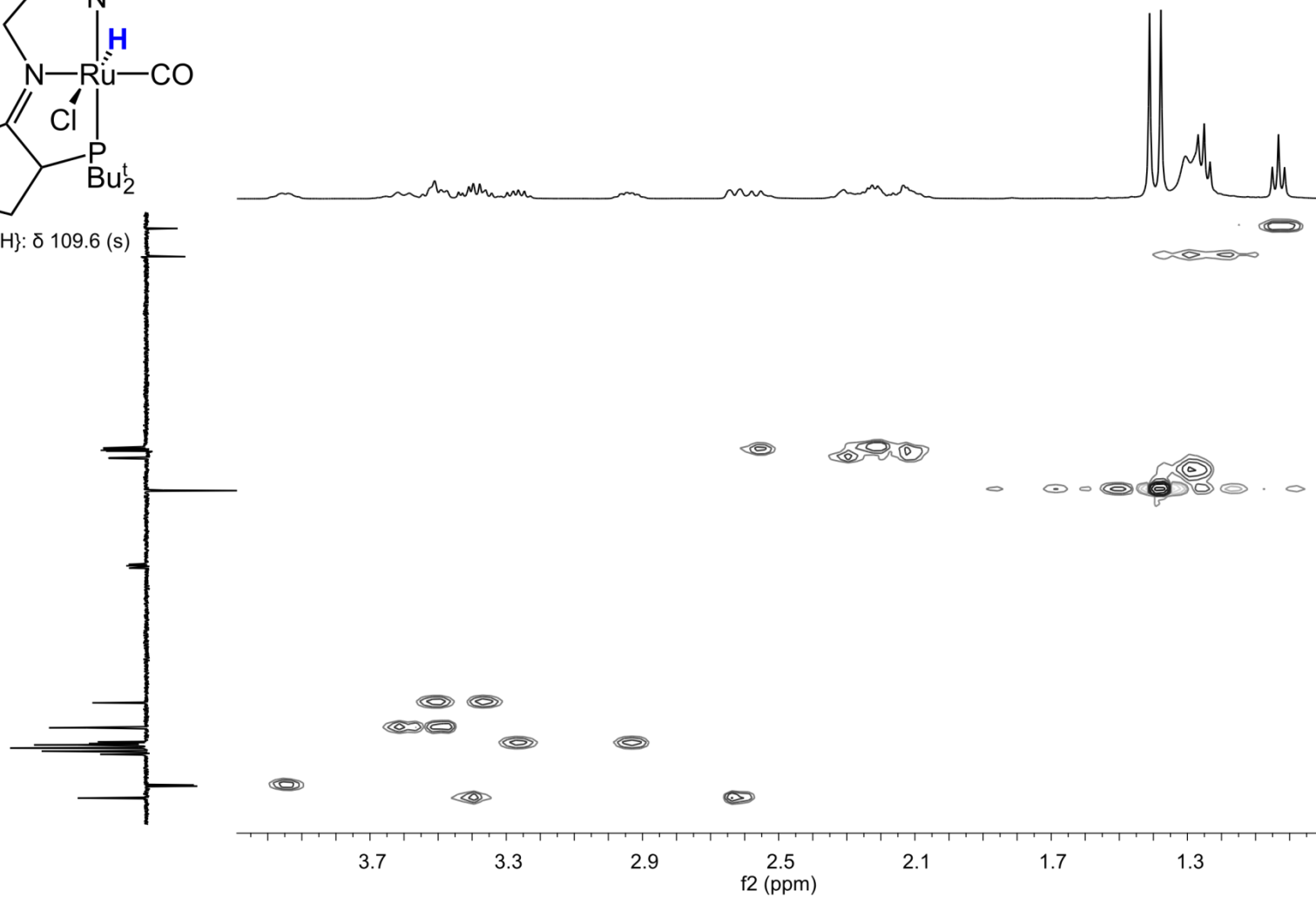
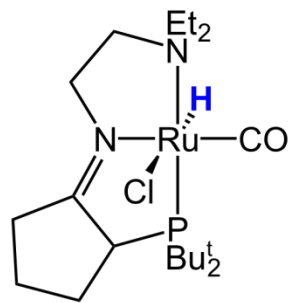


Figure S21: ¹H-¹³C HSQC of **3a** taken at 298 K in CD₂Cl₂.



³¹P{¹H}: δ 109.6 (s)

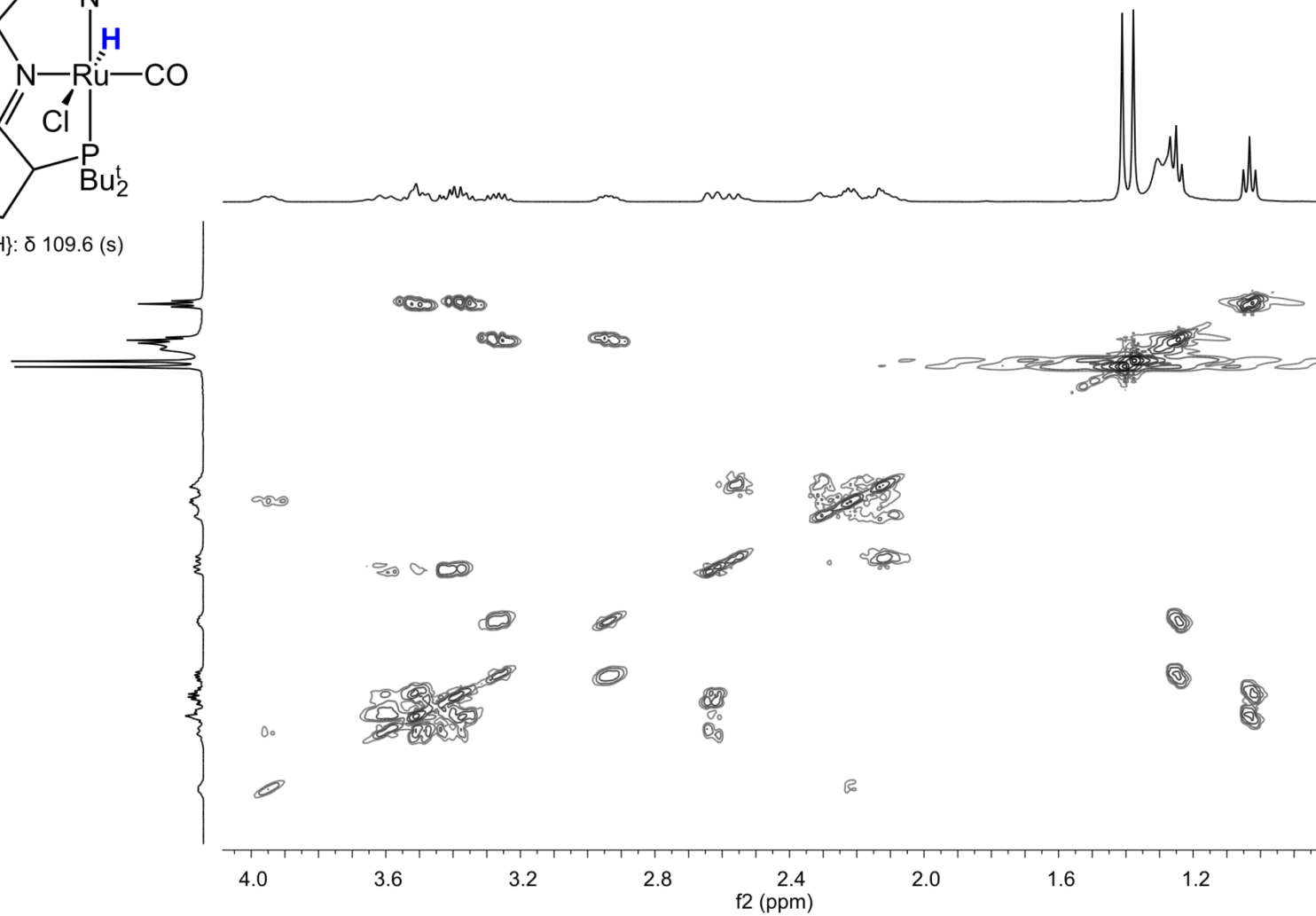


Figure S22: ¹H-¹H COSY of **3a** taken at 298 K in CD₂Cl₂.

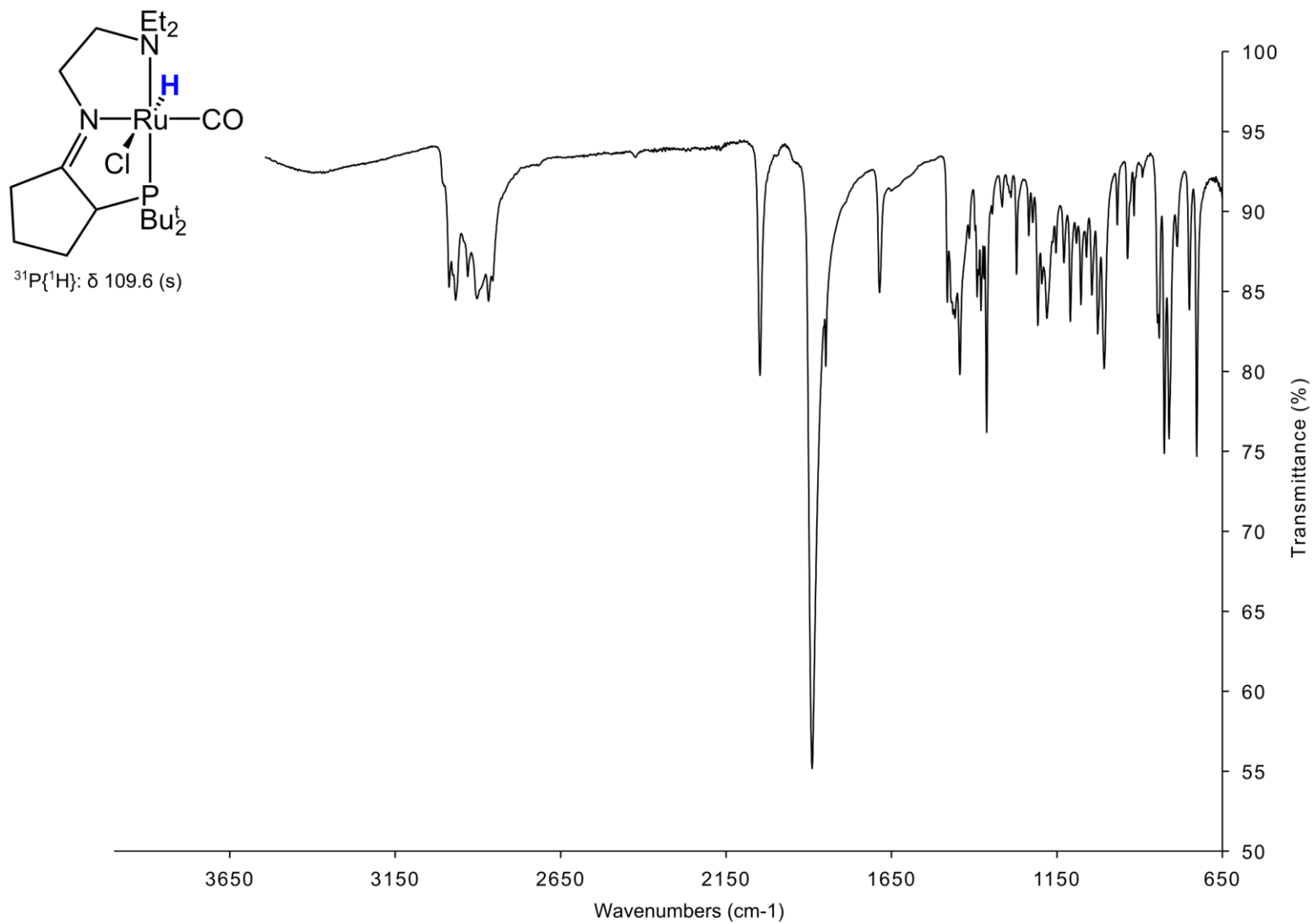


Figure S23: ATR-FTIR of **3a**.

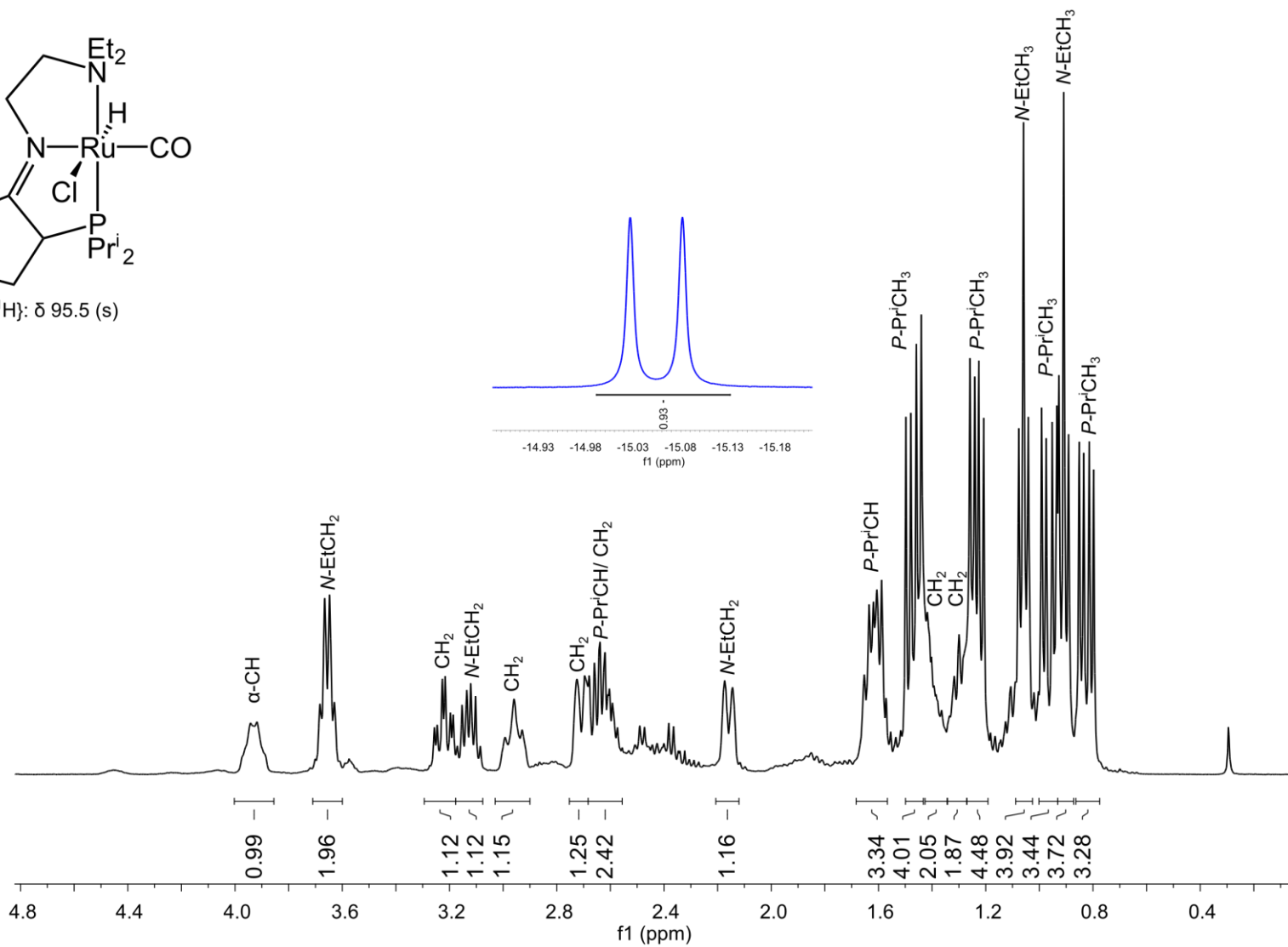
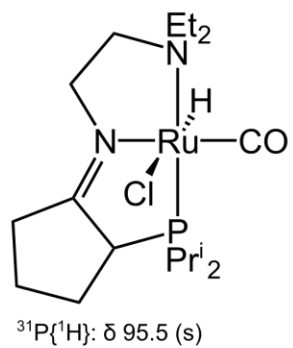


Figure S24: ^1H NMR of **3b** taken at 400.0 MHz at 298 K in C_6D_6 .

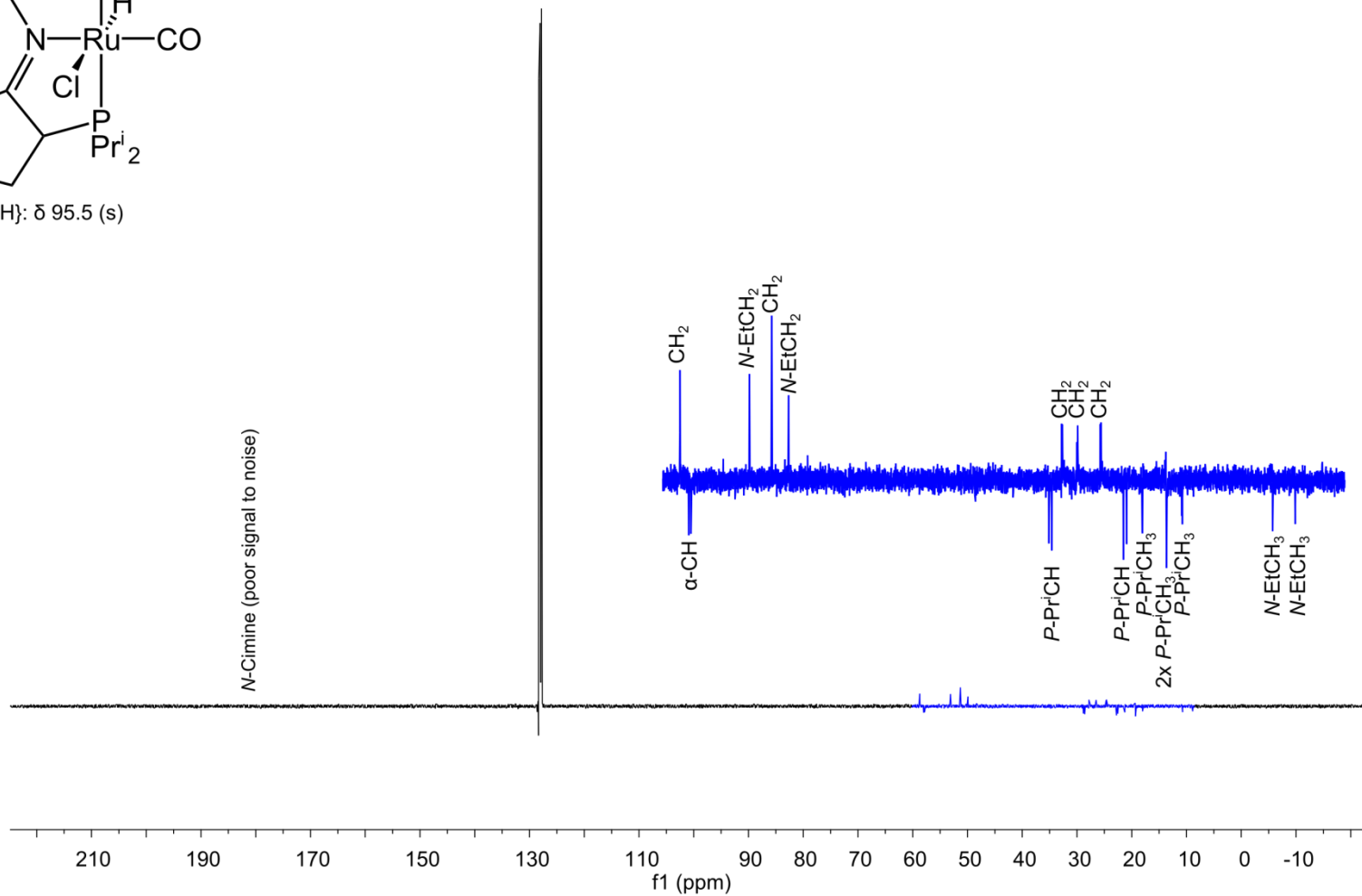
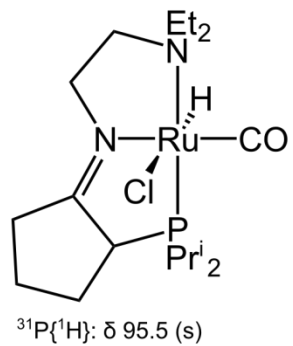
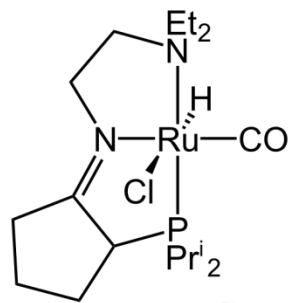


Figure S25: ^{13}C APT NMR of **3b** taken at 100.6 MHz at 298 K in C_6D_6 .



³¹P{¹H}: δ 95.5 (s)

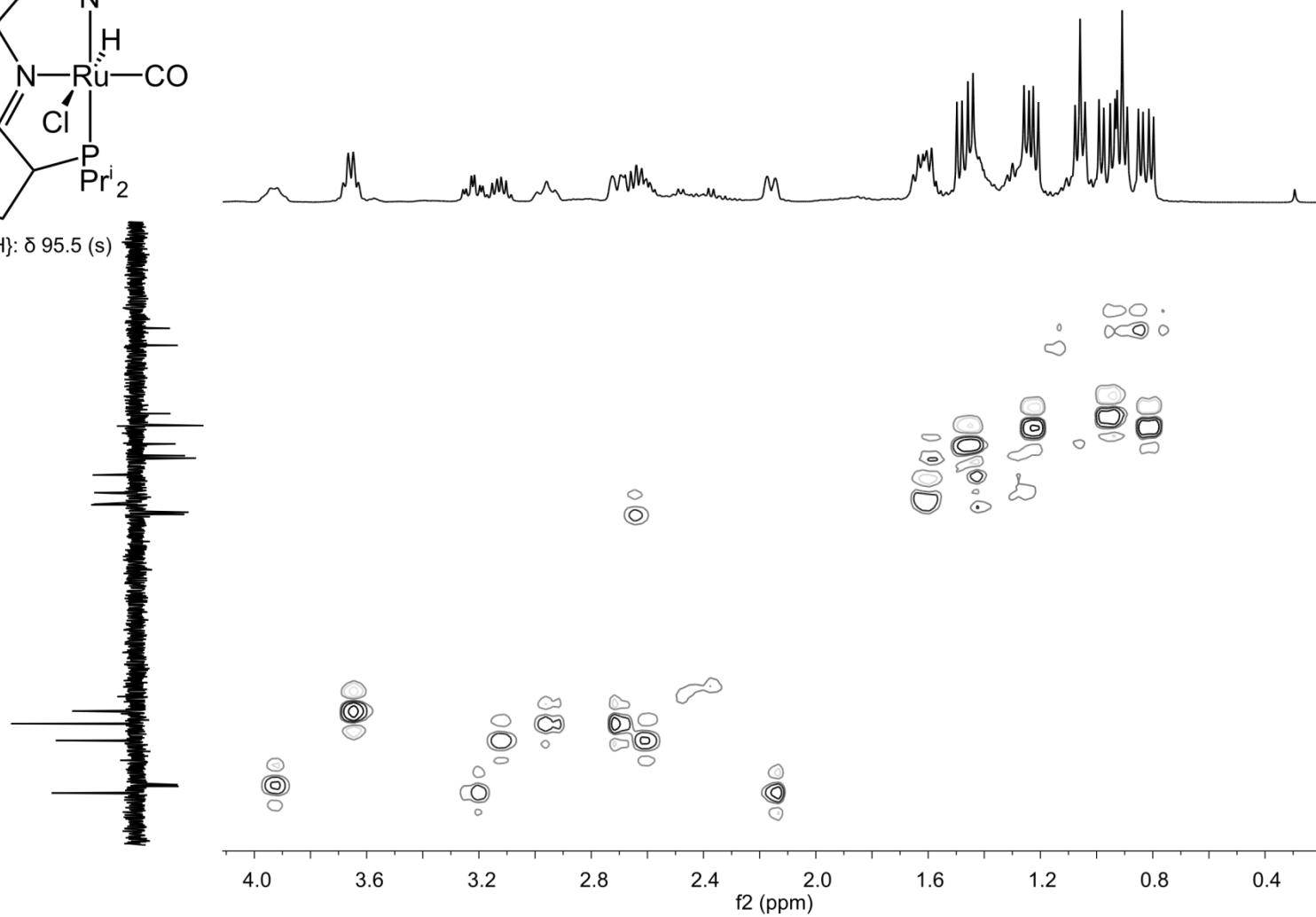
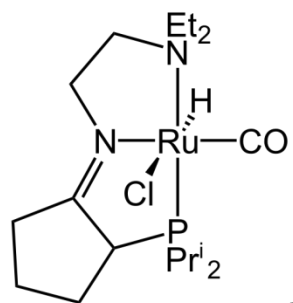


Figure S26: ¹H-¹³C HSQC of **3b** taken at 298 K in C₆D₆.



³¹P{¹H}: δ 95.5 (s)

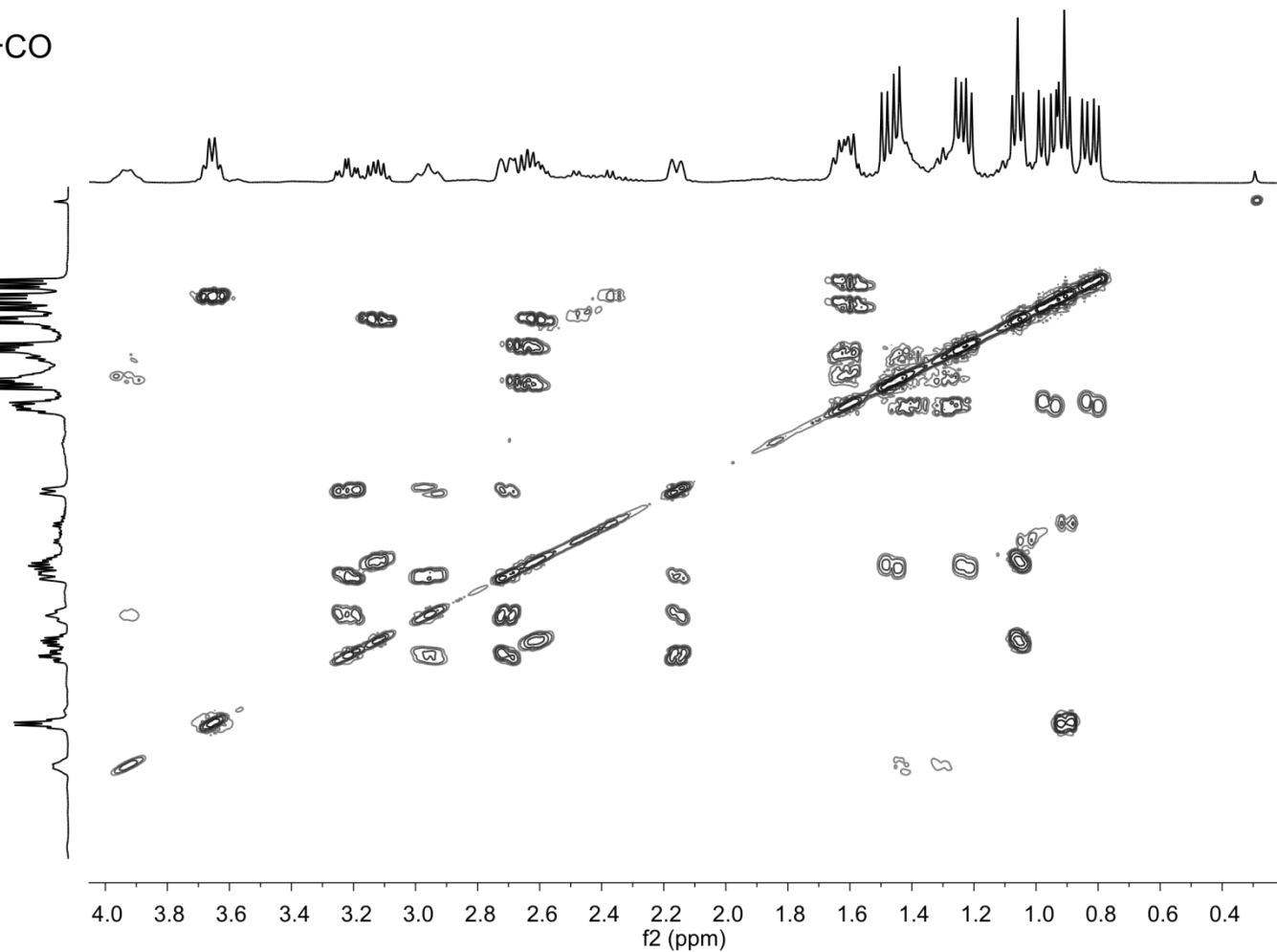


Figure S27: ¹H-¹H COSY of **3b** taken at 298 K in C₆D₆.

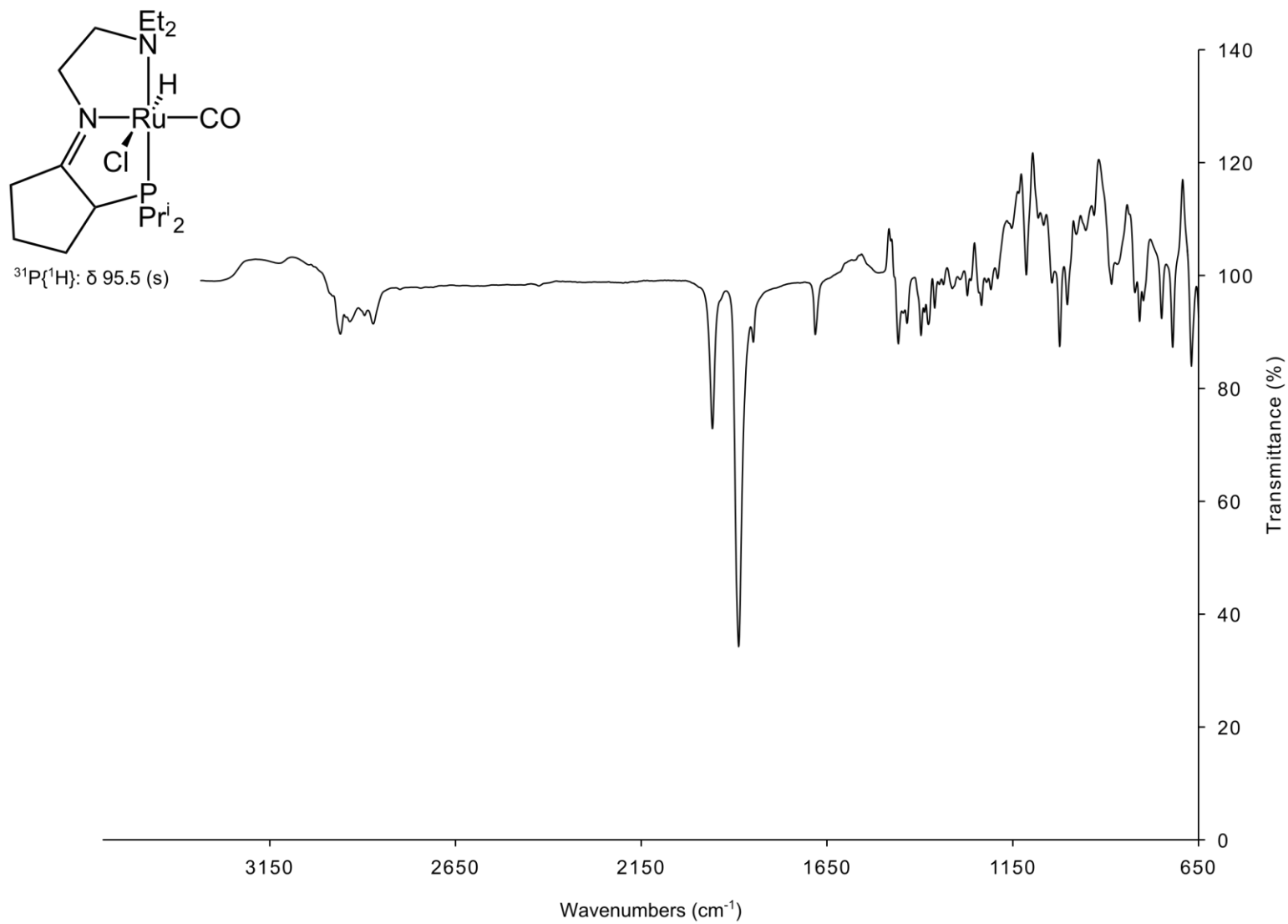
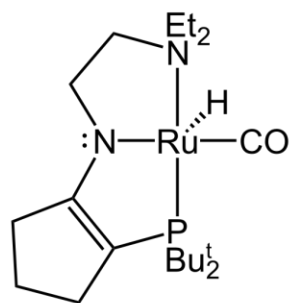


Figure S28: ATR-FTIR of **3b**.



$^{31}\text{P}\{^1\text{H}\}$: δ 92.3 (s)

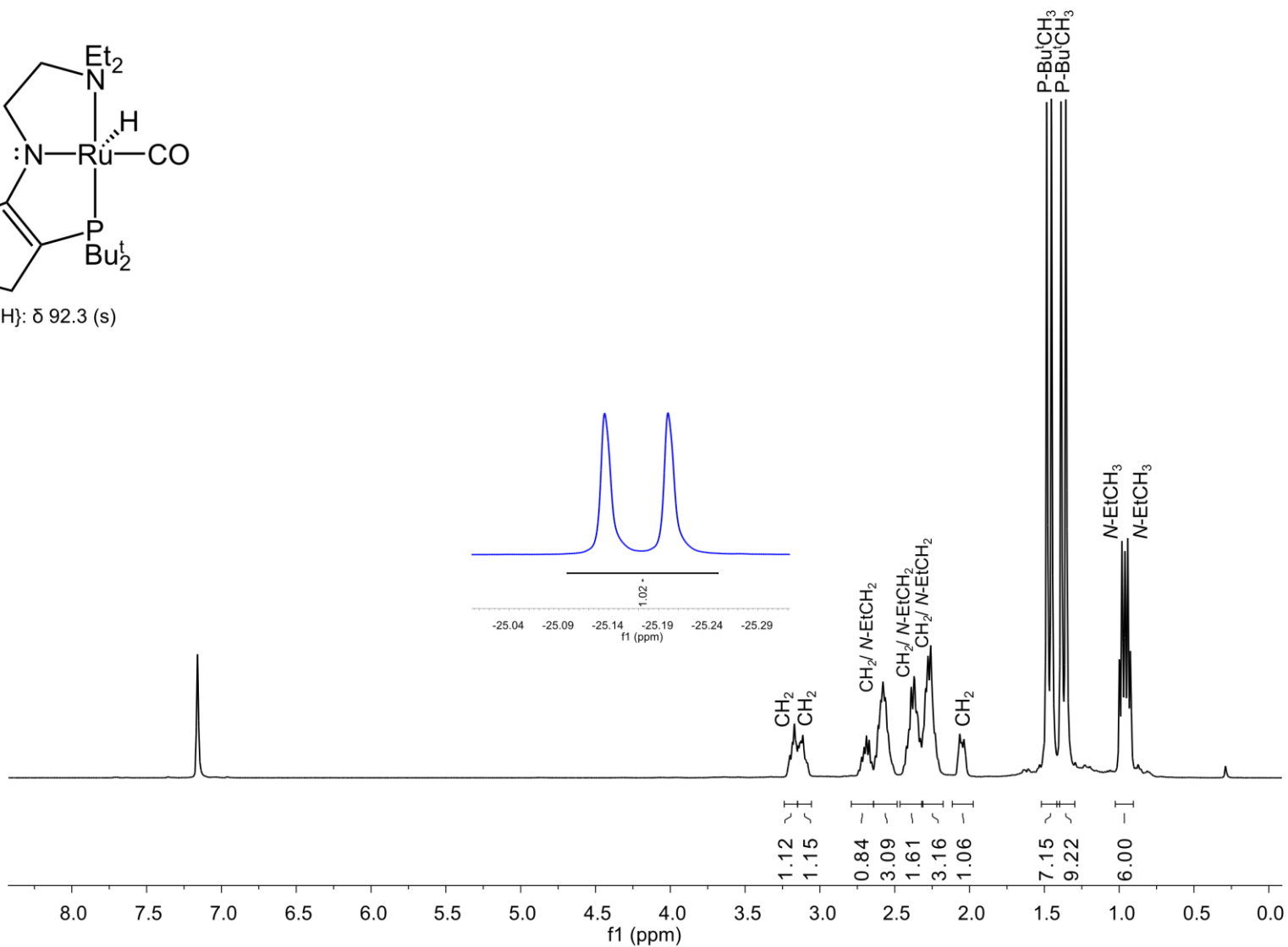


Figure S29: ^1H NMR of **4a** taken at 400.0 MHz at 298 K in C_6D_6 .

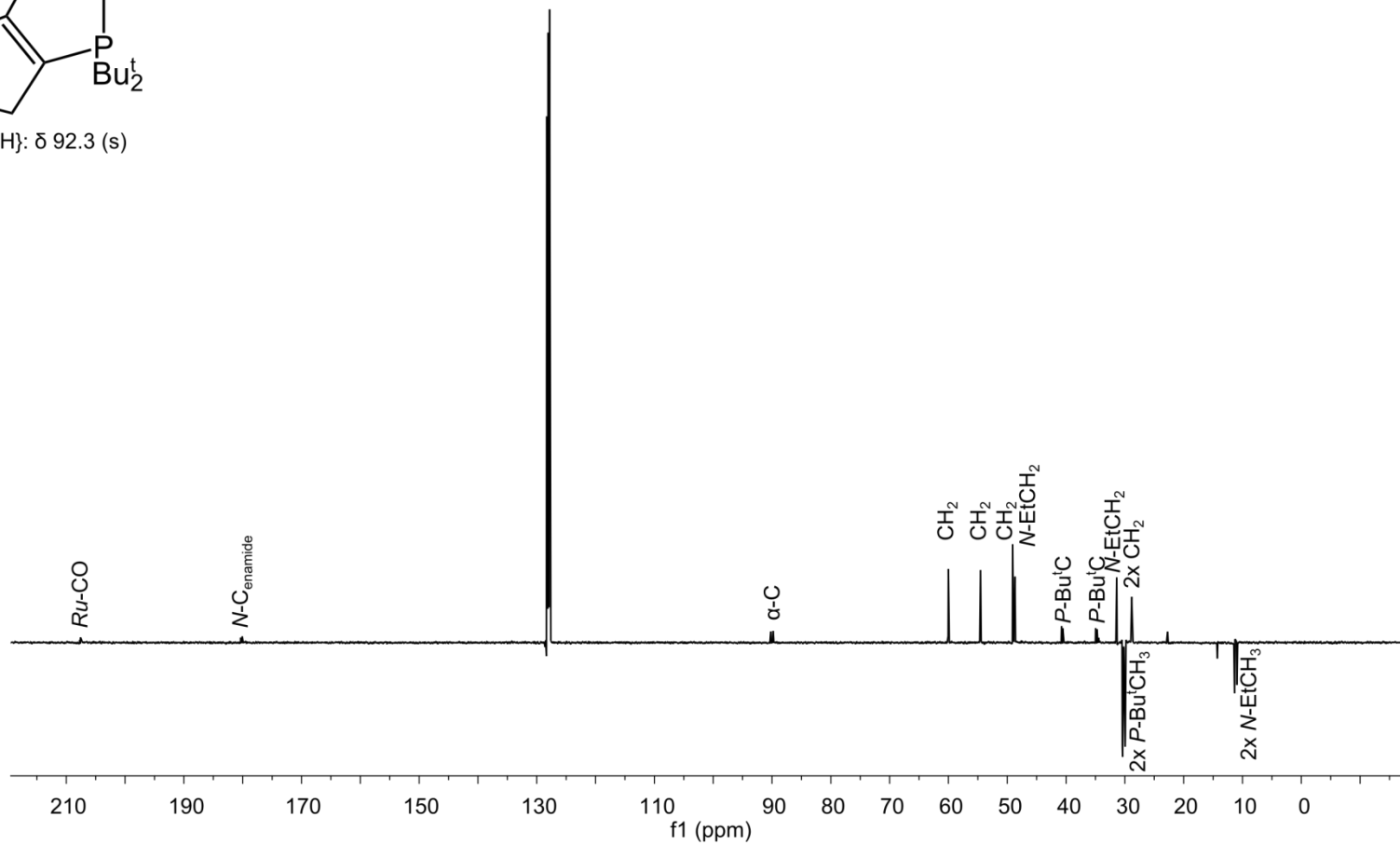
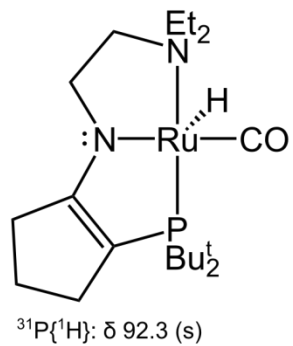


Figure S30: ^{13}C APT NMR of **4a** taken at 100.6 MHz at 298 K in C_6D_6 .

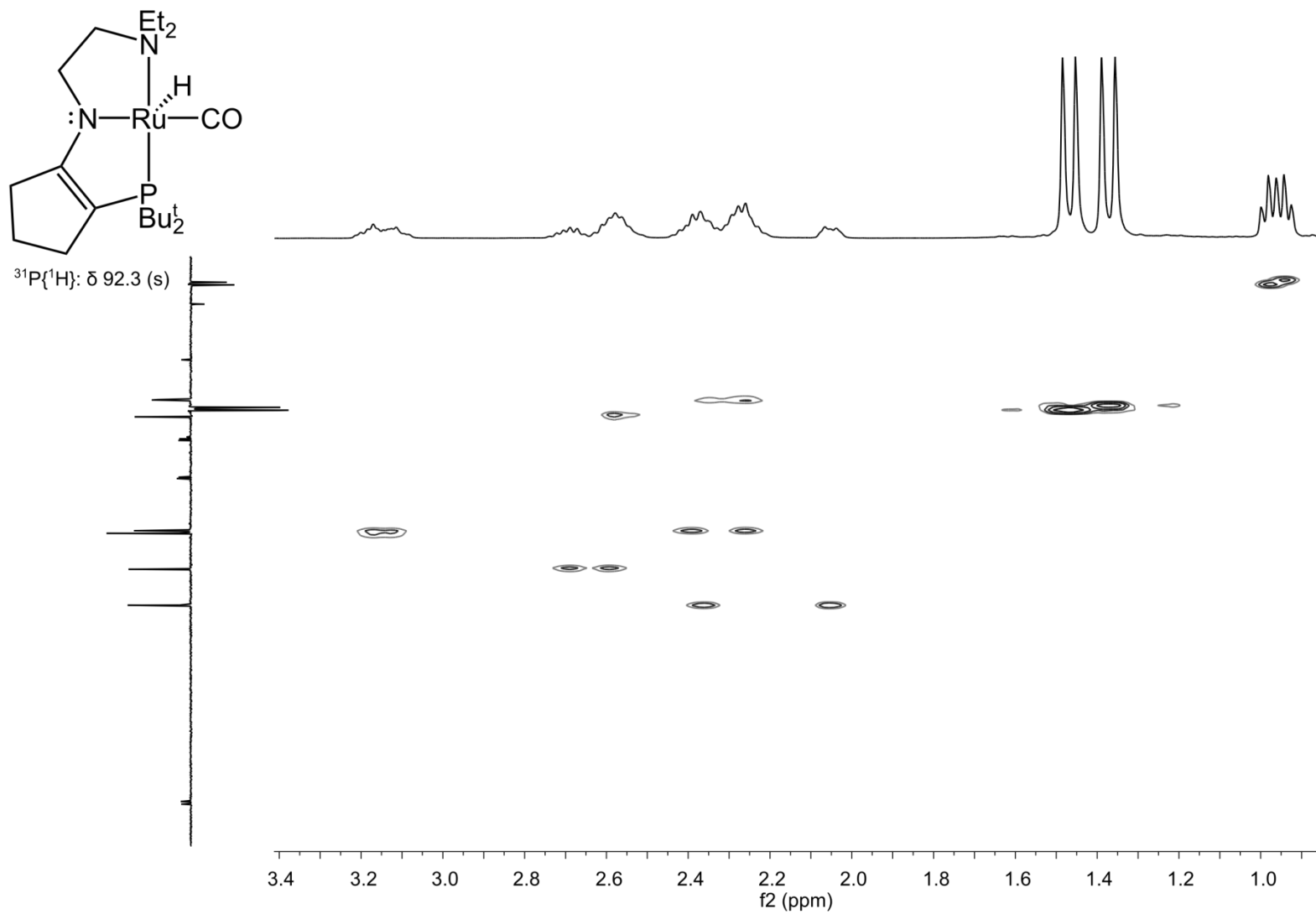


Figure S31: ^1H - ^{13}C HSQC of **4a** taken at 298 K in C_6D_6 .

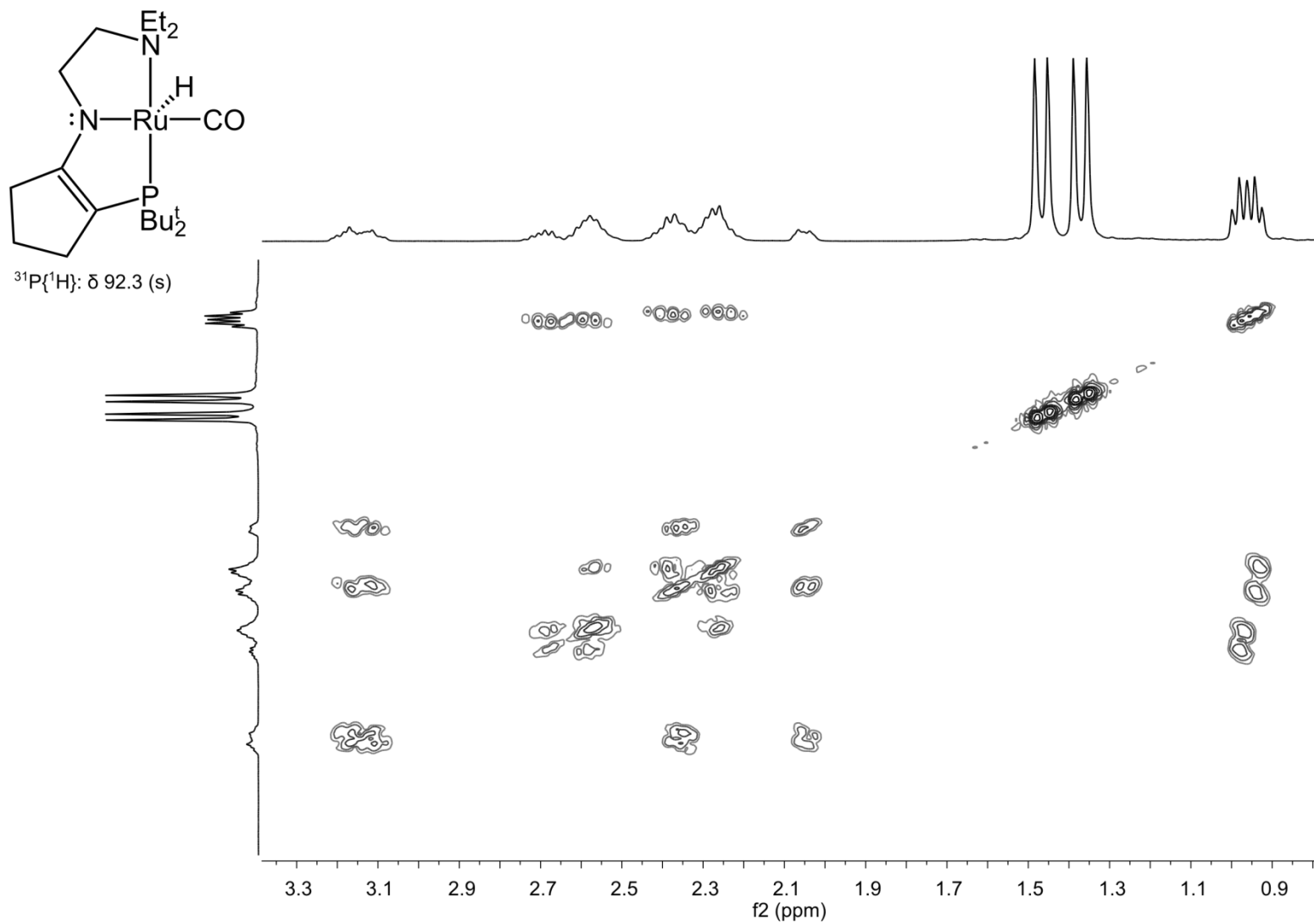


Figure S32: ^1H - ^1H COSY of **4a** taken at 298 K in C_6D_6 .

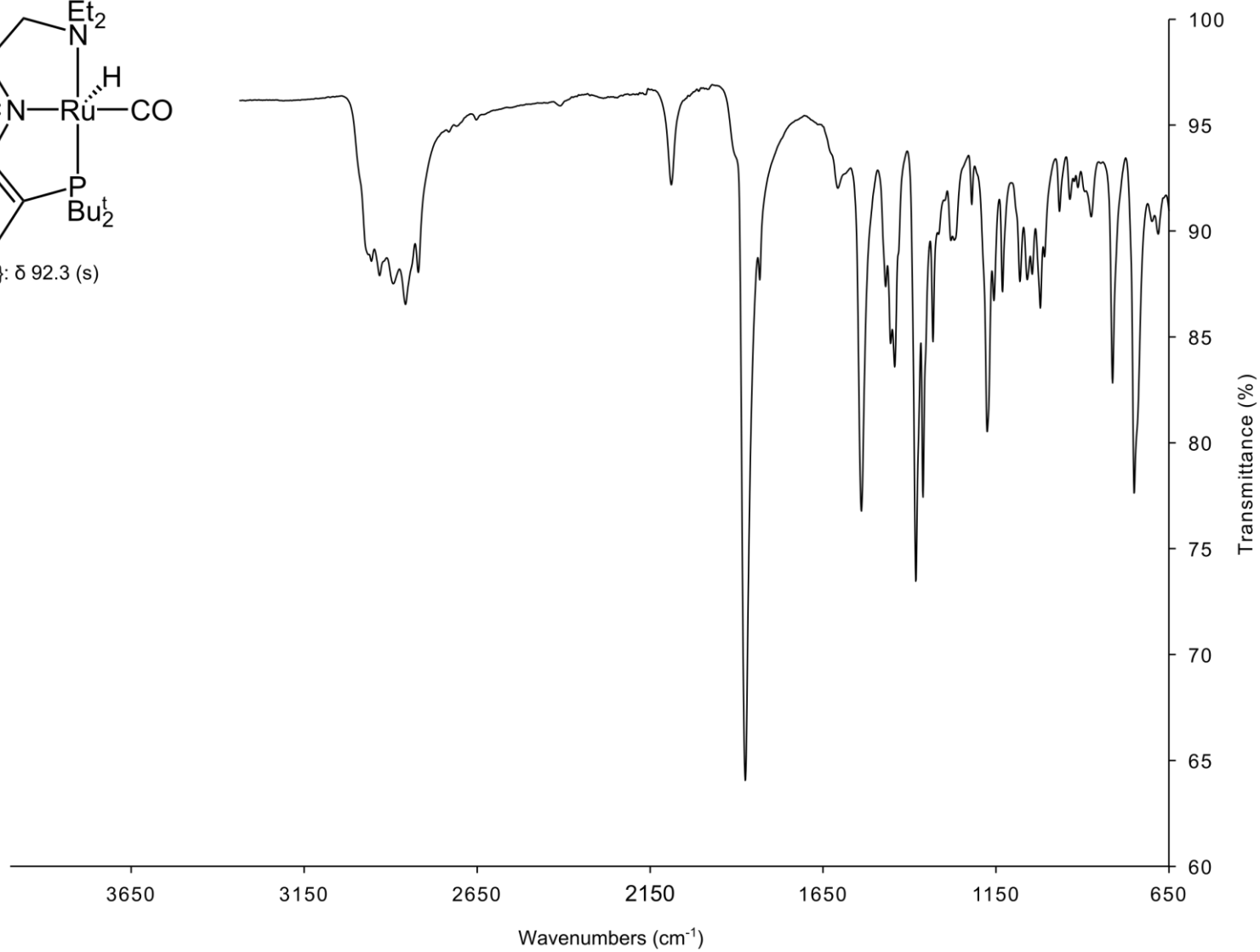
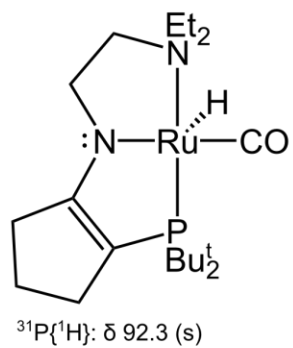


Figure S33: ATR-FTIR of **4a**.

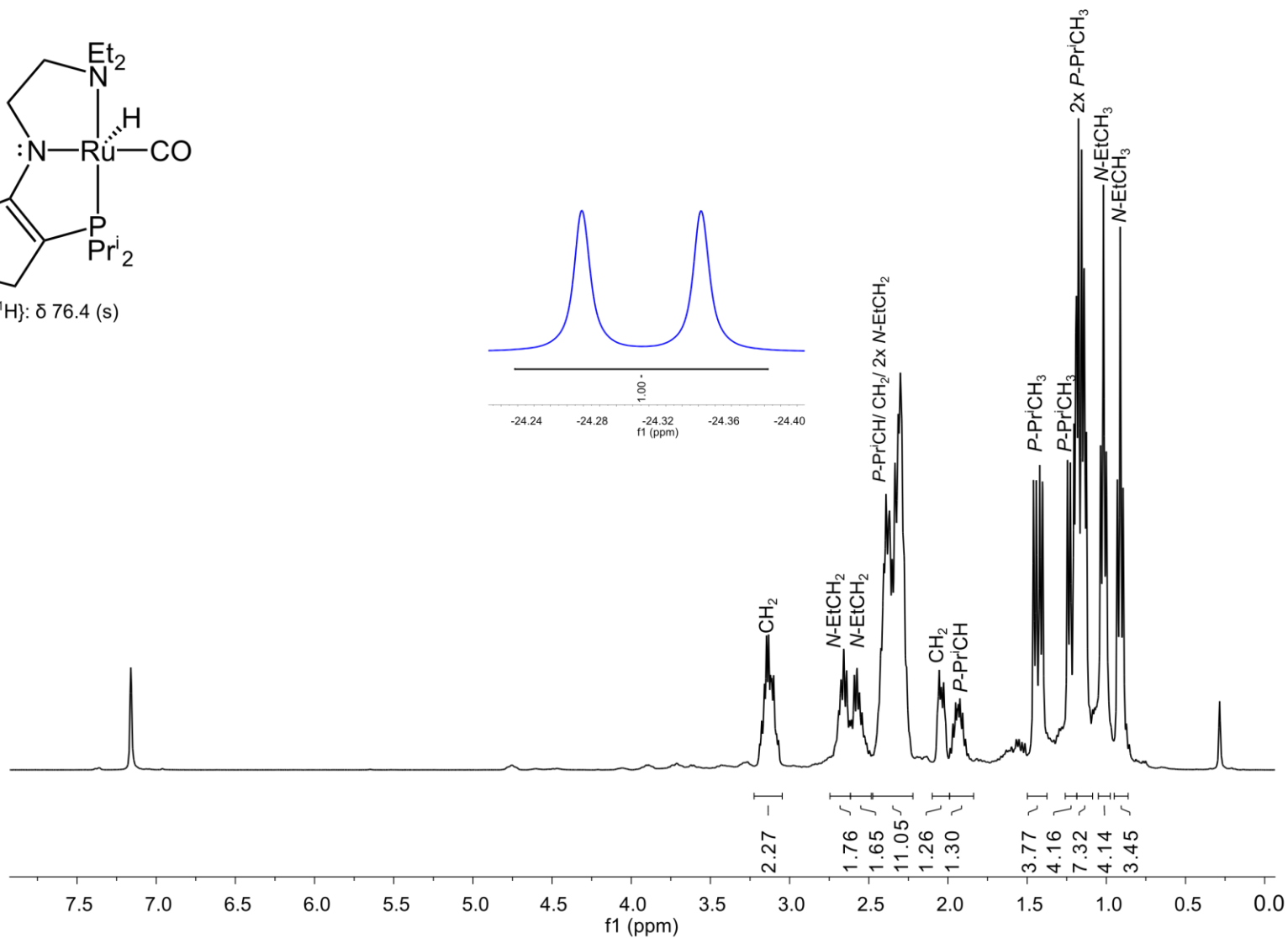
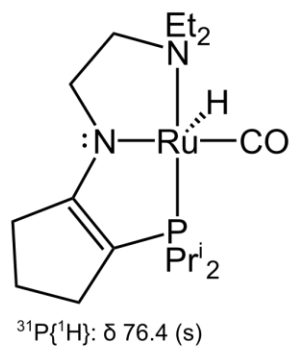


Figure S34: ^1H NMR of **4b** taken at 400.0 MHz at 298 K in C_6D_6 .

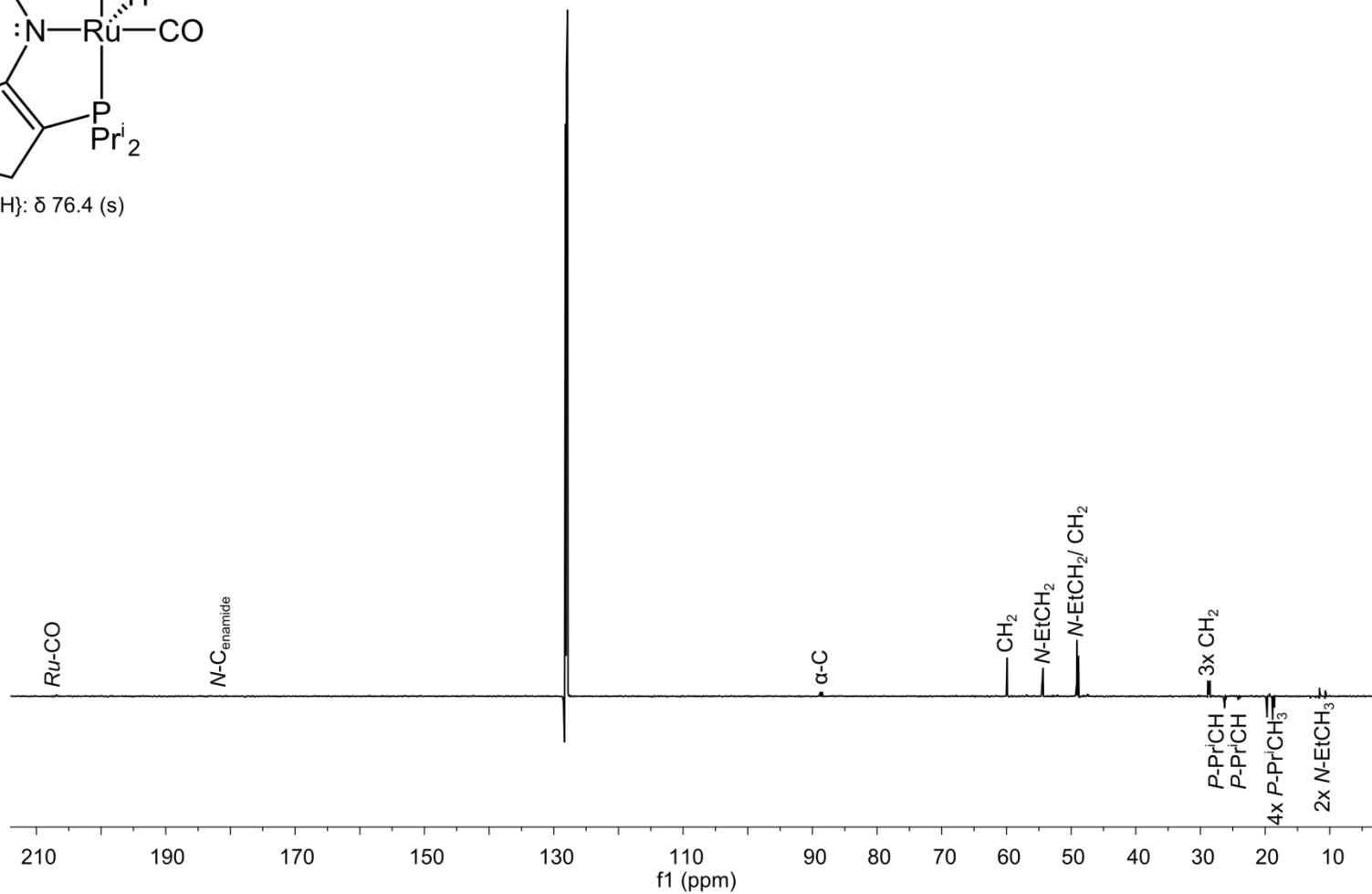
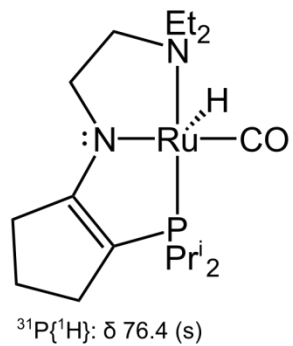


Figure S35: ^{13}C APT NMR of **4b** taken at 100.6 MHz at 298 K in C_6D_6 .

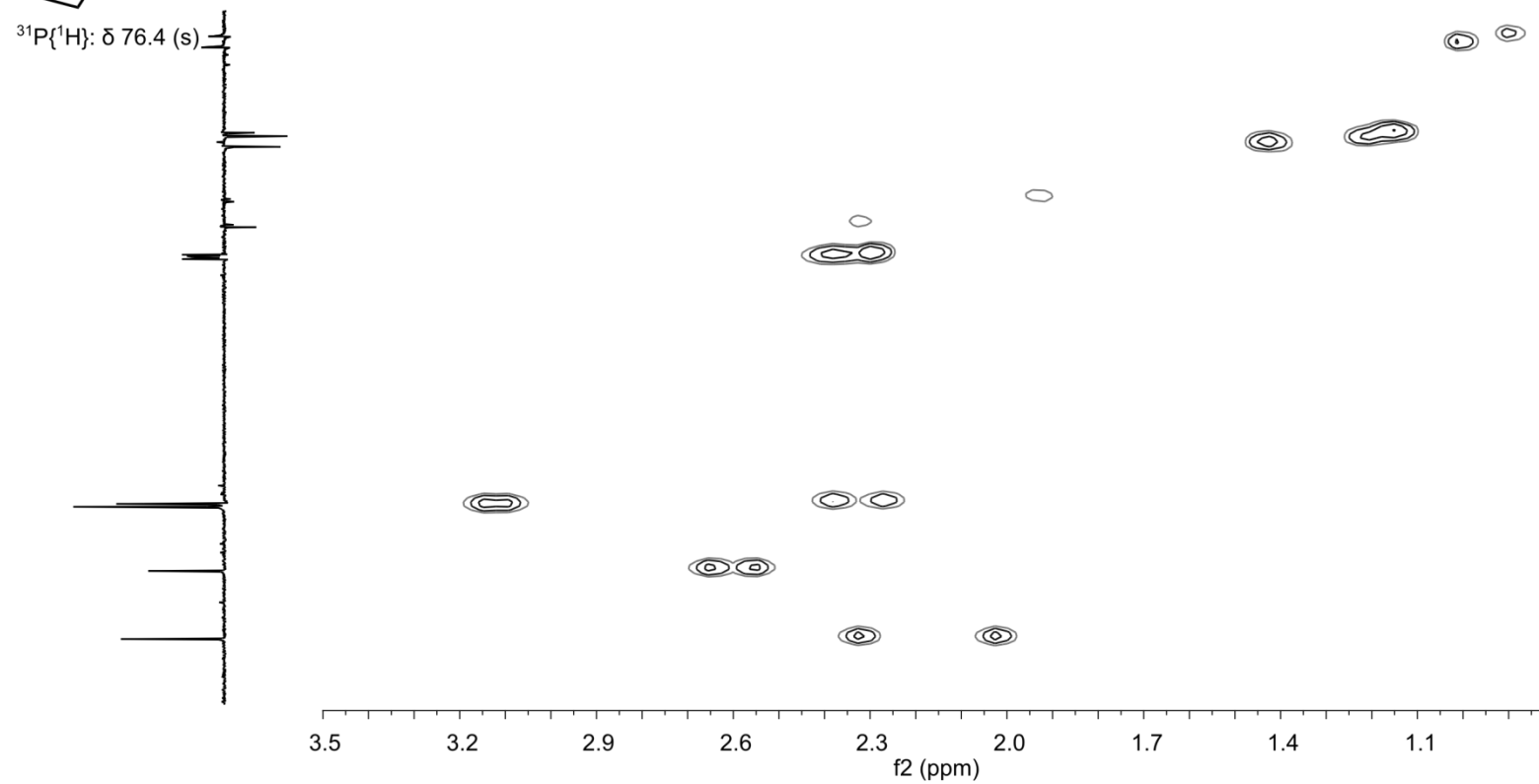
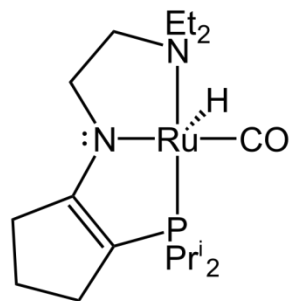
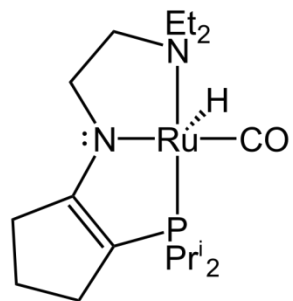


Figure S36: ¹H-¹³C HSQC of **4b** taken at 298 K in C₆D₆.



³¹P{¹H}: δ 76.4 (s)

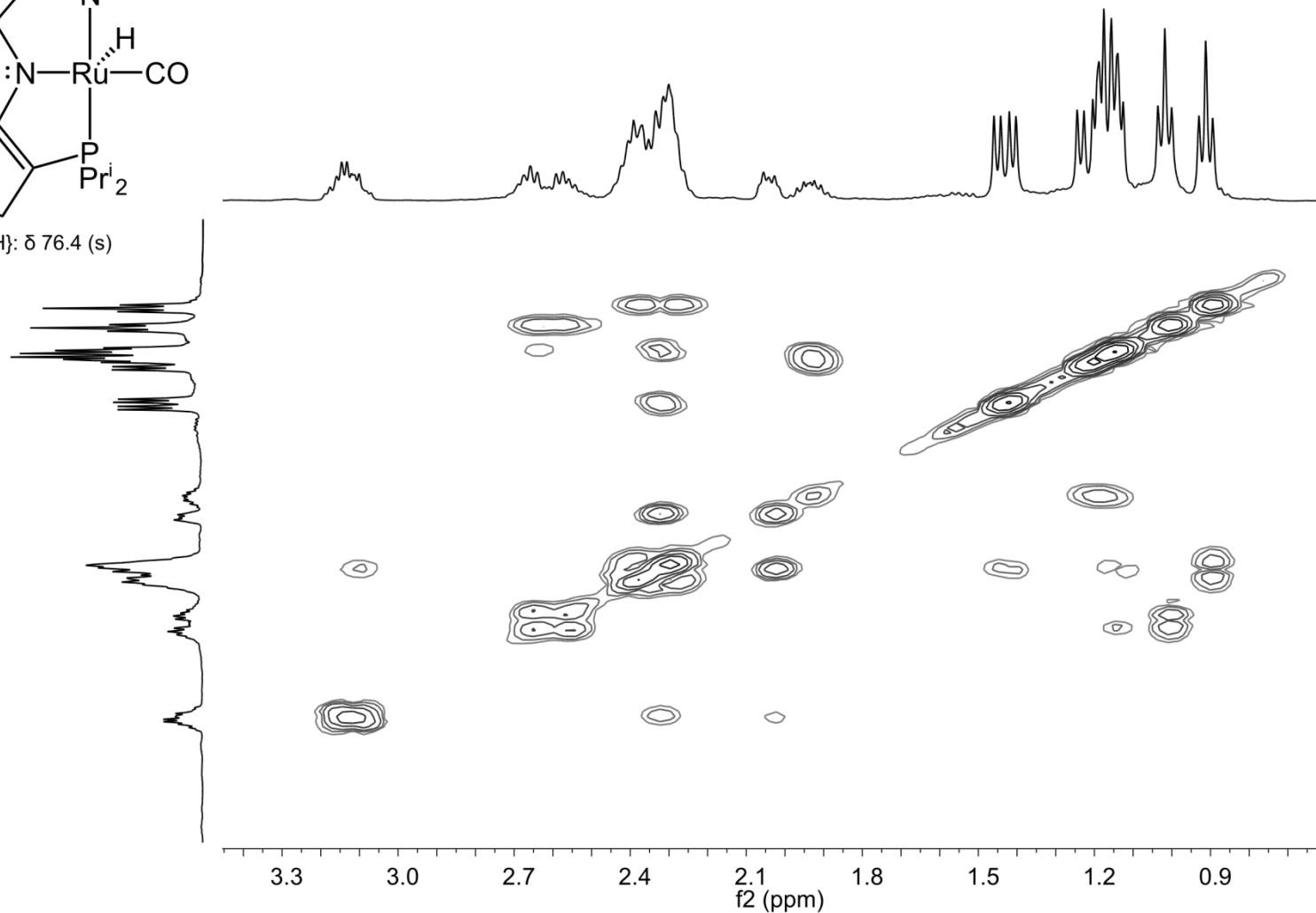


Figure S37: ¹H-¹H COSY of **4b** taken at 298 K in C₆D₆.

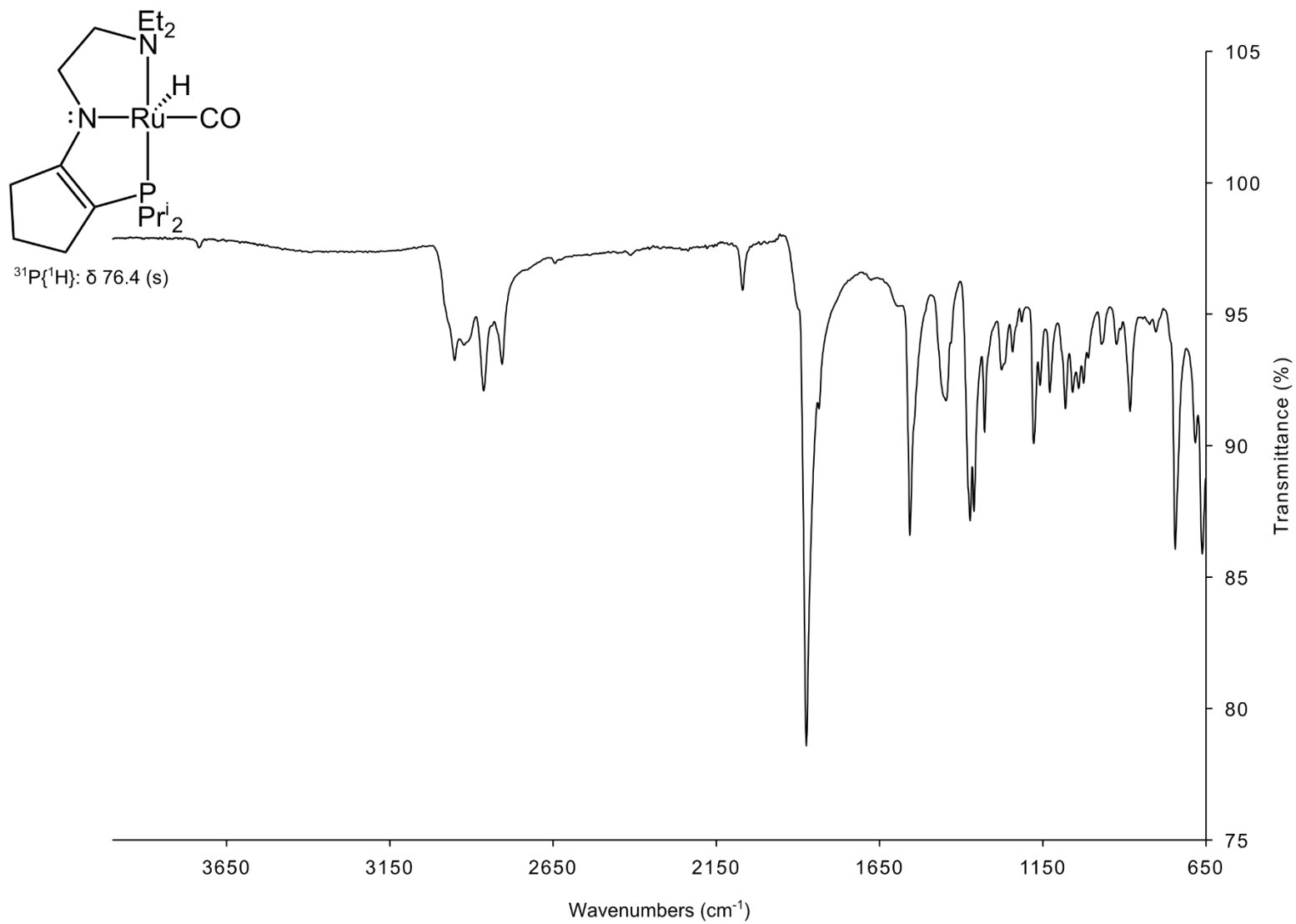


Figure S38: ATR-FTIR of **4b**.

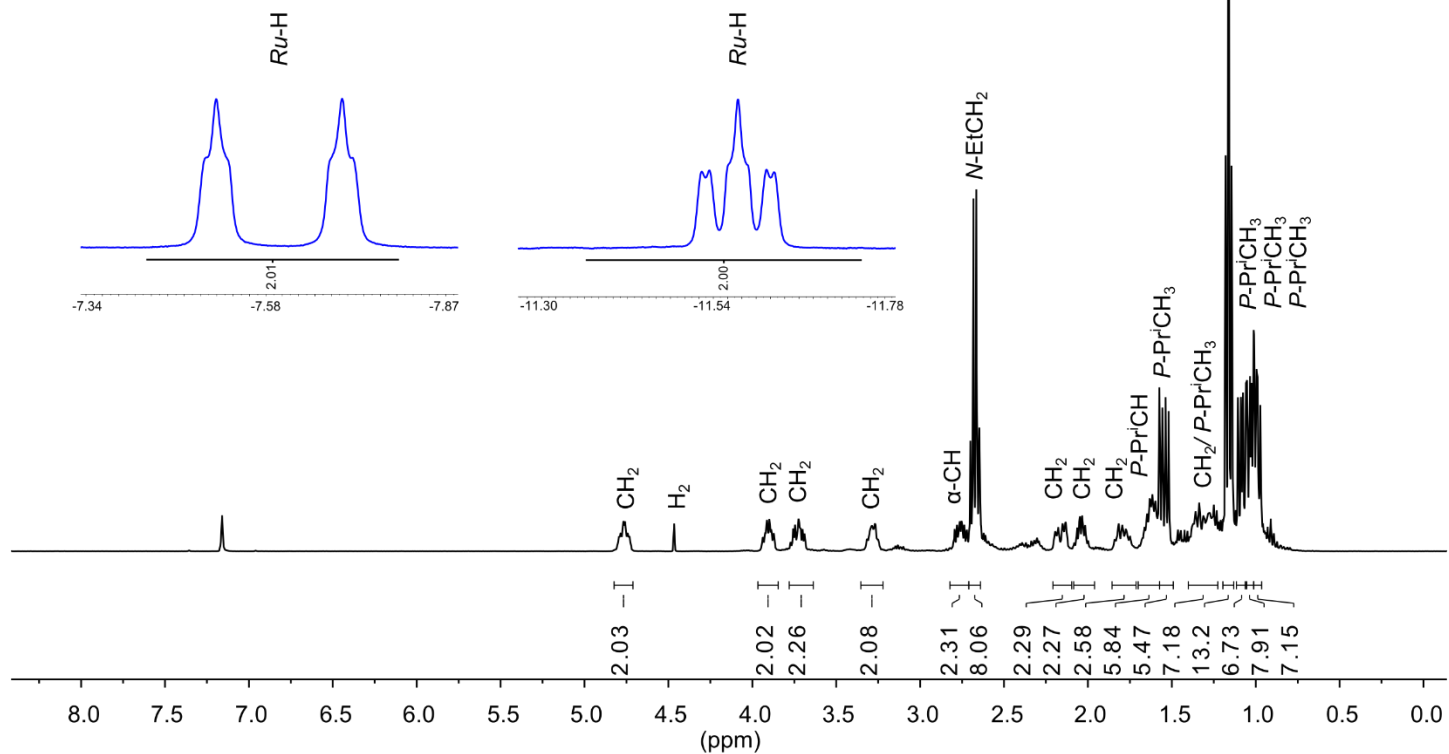
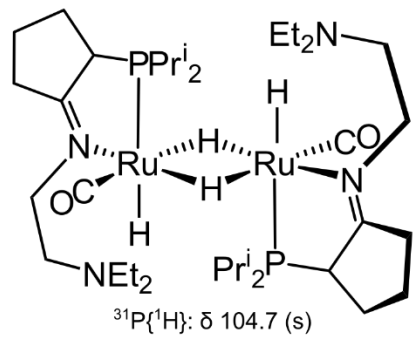


Figure S39: ^1H NMR of **5** taken at 400.0 MHz at 298 K in C_6D_6 .

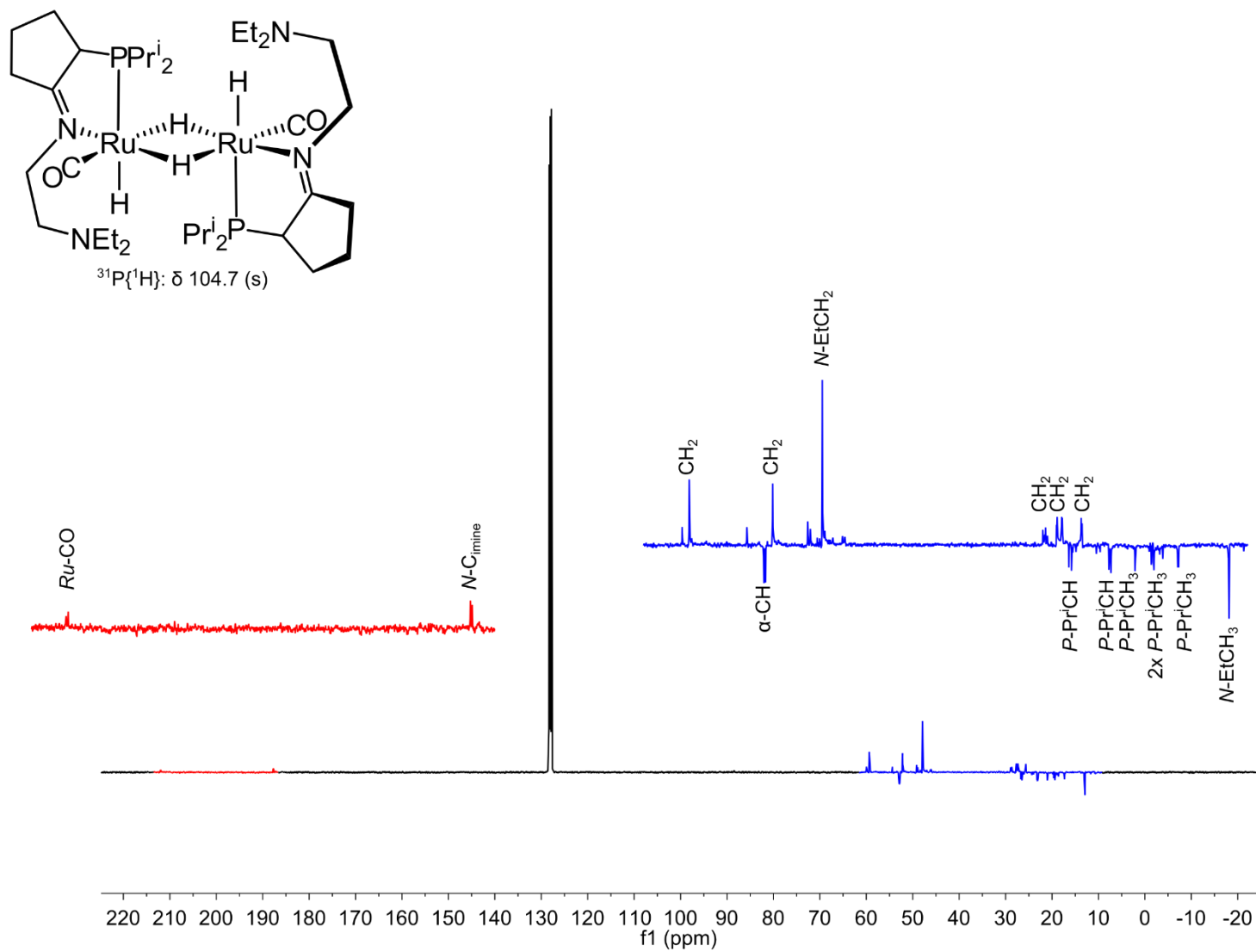


Figure S40: ¹³C APT NMR of **5** taken at 100.6 MHz at 298 K in C₆D₆.

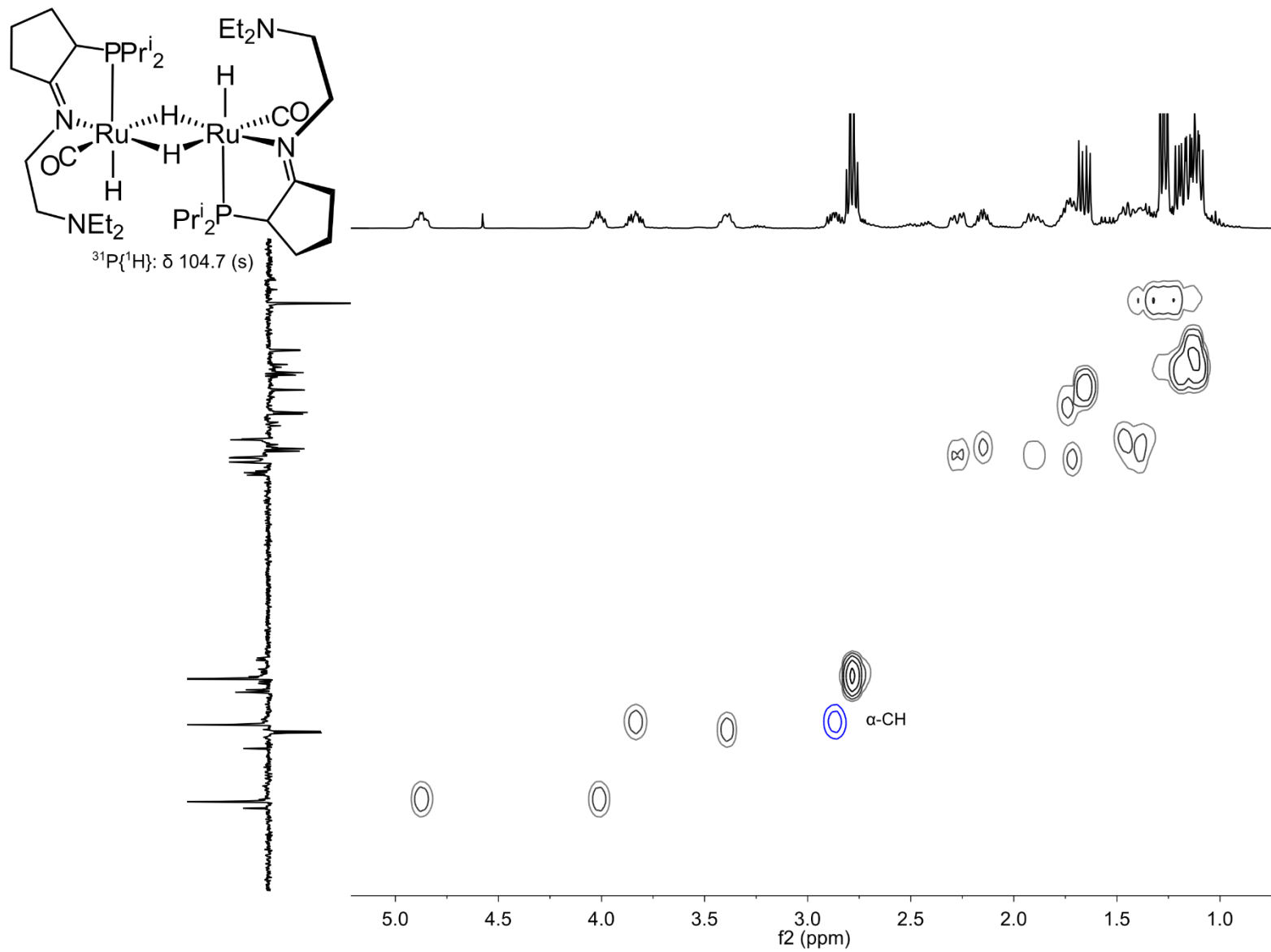


Figure S41: ^1H - ^{13}C HSQC of **5** taken at 298 K in C_6D_6 .

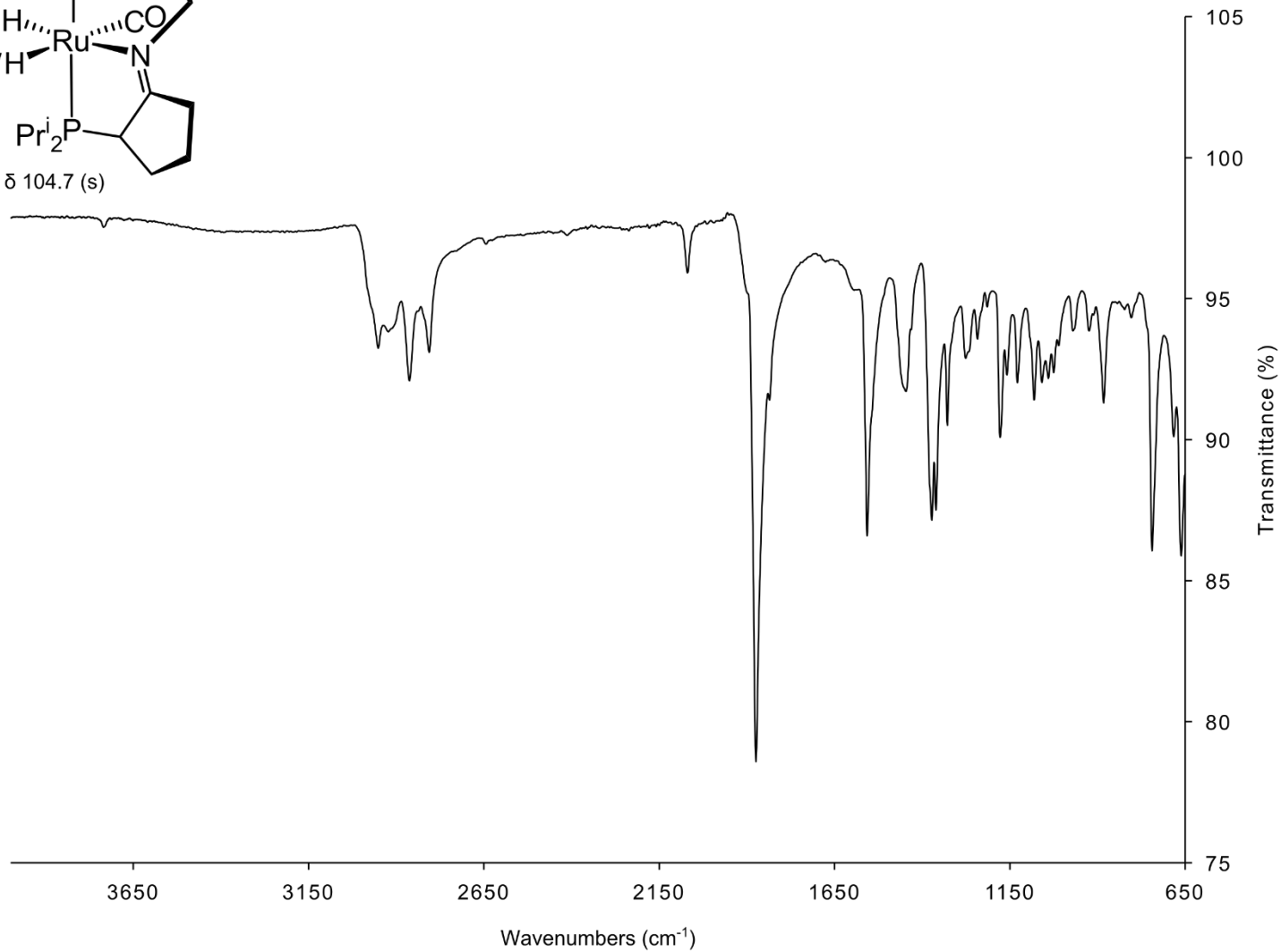
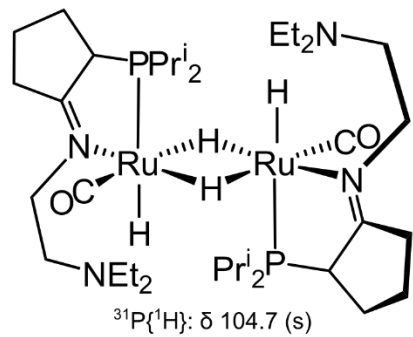


Figure S42: ATR-FTIR of **5**.